

ϵ_K at NNLO: The Charm-Top-Quark Contribution

Joachim Brod^{a,b,c} and Martin Gorbahn^{b,c}

^aInstitut für Theoretische Teilchenphysik,
Universität Karlsruhe, D-76128 Karlsruhe, Germany

^bExcellence Cluster Universe, Technische Universität München,
Boltzmannstraße 2, D-85748 Garching

^cInstitute for Advanced Study, Technische Universität München,
Arcisstraße 21, D-80333 München, Germany

Abstract

We perform a next-to-next-to-leading order (NNLO) QCD analysis of the charm-top-quark contribution η_{ct} to the effective $|\Delta S| = 2$ Hamiltonian in the Standard Model. η_{ct} represents an important part of the short distance contribution to the parameter ϵ_K . We calculate the three-loop anomalous dimension of the leading operator \tilde{Q}_{S2} , the three-loop mixing of the current-current and penguin operators into \tilde{Q}_{S2} , and the corresponding two-loop matching conditions at the electroweak, the bottom-quark, and the charm-quark scale. As our final numerical result we obtain $\eta_{ct} = 0.494 \pm 0.046$, which is roughly 7% larger than the next-to-leading-order (NLO) value $\eta_{ct}^{\text{NLO}} = 0.455 \pm 0.069$. This results in a prediction for $|\epsilon_K| = (1.99 \pm 0.25) \times 10^{-3}$, which corresponds to an enhancement of approximately 3.3% with respect to the value obtained using η_{ct}^{NLO} .

1 Introduction

Indirect CP violation in the neutral Kaon system was discovered by Christenson, Cronin, Fitch and Turlay in 1964, who observed the decay of a K_L into two pions [1]. This decay would be forbidden in the case of exact CP symmetry. The parameter ϵ_K measures indirect CP violation and is defined by

$$\epsilon_K = \frac{\mathcal{A}(K_L \rightarrow (\pi\pi)_{I=0})}{\mathcal{A}(K_S \rightarrow (\pi\pi)_{I=0})} \quad (1.1)$$

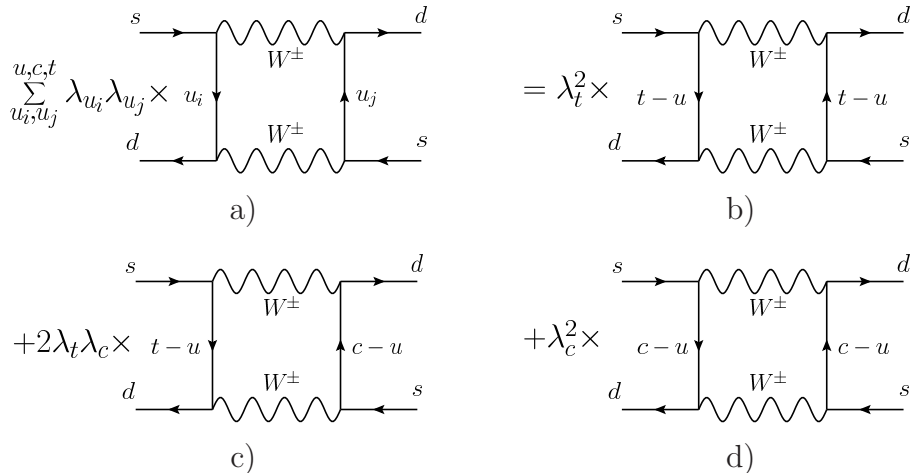


Figure 1: The $\Delta S = 2$ box-type diagram with internal up, charm, and top contributions is expressed as a sum of box-type diagrams proportional to λ_t^2 , λ_c^2 , and $\lambda_t\lambda_c$, respectively, using the GIM mechanism.

via the ratio of the respective decay amplitudes of a K_L and a K_S decaying into a two-pion state of isospin zero in such a way that direct CP violation is absent to a good approximation.

The parameter ϵ_K is measured with high accuracy: The value quoted by the Particle Data Group is $\epsilon_K = (2.229 \pm 0.012) \times 10^{-3} \times e^{i(43.5 \pm 0.7)^\circ}$ [2]. Whereas until about a decade ago the numerical value of ϵ_K was used as an input to determine the Standard Model parameters, nowadays it plays a central role in constraining models of new physics: The near diagonality of the Cabibbo-Kobayashi-Maskawa (CKM) matrix leads to a suppression in the Standard Model, while ϵ_K can be predicted very reliably.

For the theoretical prediction it is useful to express ϵ_K in terms of $\langle \bar{K}^0 | \mathcal{H}_{f=3}^{|\Delta S|=2} | K^0 \rangle = 2M_K M_{12}^*$, the matrix element of the $\Delta S = 2$ effective Hamiltonian, and write:

$$\epsilon_K = e^{i\phi_\epsilon} \sin \phi_\epsilon \left(\frac{\text{Im}(M_{12}^*)}{\Delta M_K} + \xi \right). \quad (1.2)$$

Here M_K is the neutral Kaon mass and ΔM_K the Kaon mass difference, the phase of ϵ_K is $\phi_\epsilon = 43.5(7)^\circ$ [2] and $\xi = \text{Im}A_0/\text{Re}A_0 \simeq 0$ is the imaginary part divided by the real part of the isospin zero amplitude $A_0 = \mathcal{A}(K_S \rightarrow (\pi\pi)_{I=0})$. The ratio $\kappa_\epsilon = |\epsilon_K^{SM}/\epsilon_K(\phi_\epsilon = 45^\circ, \xi = 0)|$ encompasses the change of $|\epsilon_K|$ if the values $\phi_\epsilon = 45^\circ$ and $\xi = 0$ are used in (1.2), as has been done in most of the older analyses, instead of the exact values. The authors of Reference [3] give the value of $\kappa_\epsilon = 0.94 \pm 0.02$ in the Standard Model, including in their analysis also contributions of higher-dimensional operators to the absorptive and dispersive part of the $K^0 - \bar{K}^0$ mixing amplitude.

The box diagram of Fig. 1a gives the leading contribution to the effective Hamiltonian $\mathcal{H}_{f=3}^{|\Delta S|=2}$ and the parameter M_{12} . It is proportional to a sum of loop functions times CKM

factors, which, using $\lambda_i = V_{is}^* V_{id}$ and $x_i = m_i^2/M_W^2$ we can write as:

$$\sum_{u_i, u_j \in \{u, c, t\}} \lambda_{u_i} \lambda_{u_j} \tilde{S}(x_{u_i}, x_{u_j}) =: \lambda_t^2 S(x_t) + \lambda_c^2 S(x_c) + 2\lambda_c \lambda_t S(x_t, x_c), \quad (1.3)$$

where \tilde{S} denotes the contributions of the individual box diagrams. After the GIM mechanism has been used to eliminate $\lambda_u = -\lambda_t - \lambda_c$ it comprises the top-quark contribution – proportional to λ_t^2 (Fig. 1b), the charm-quark contribution – proportional to λ_c^2 (Fig. 1c), and the charm-top-quark contribution (Fig. 1d) – proportional to $\lambda_c \lambda_t$. The resulting loop functions $S(x_i, x_j) = \tilde{S}(x_i, x_j) - \tilde{S}(x_i, 0) - \tilde{S}(0, x_j) + \tilde{S}(0, 0)$ and $S(x_i) = S(x_i, x_i)$ are suppressed by the smallness of the quark mass m_i if x_i is significantly smaller than one. This, together with the severe Cabibbo suppression of the CP violating top-quark contribution, lets all three contributions compete in size for ϵ_K :

$$\begin{aligned} \text{Im} \left(\lambda_t^2 S(x_t) + \lambda_c^2 S(x_c) + 2\lambda_t \lambda_c S(x_t, x_c) \right) \\ \simeq \mathcal{O}(\lambda^{10}) + \mathcal{O} \left(\lambda^6 \frac{m_c^2}{M_W^2} \right) + \mathcal{O} \left(\lambda^6 \frac{m_c^2}{M_W^2} \log \left(\frac{m_c}{M_W} \right) \right), \end{aligned} \quad (1.4)$$

where $\lambda = |V_{us}| \approx 0.2255$. The diagram of Figure 1a induces a large logarithm $\log m_c/M_W$ only for the charm-top-quark contribution: the large logarithm from the up quarks in Fig. 1b is power suppressed by $\Lambda_{\text{QCD}}^2/M_W^2$, while the GIM mechanism cancels a potential $\log m_c/M_W$ between the diagrams with both one up and one charm quark and the diagram with only internal charm quarks.

This can be reformulated in the language of an effective theory: the dimension-six penguin as well as the current-current operators, which have tree-level Wilson coefficients, mix only into the charm-top-quark contribution, via the bilocal mixing in Fig. 2a, yet do not induce large logarithms times tree-level Wilson coefficients proportional to λ_t^2 and λ_c^2 . QCD corrections do not change this picture but only induce the well known renormalisation group effects for the $\Delta S = 1$ effective Hamiltonian [4] and for the $\Delta S = 2$ Operator \tilde{Q}_{S2} (Fig. 2b). A leading order (LO) analysis of the charm-quark and top-quark contribution to ϵ_k then requires a one-loop calculation both for the matching at μ_W and for the running, and for the charm-quark contribution also for the matching at μ_c (Fig. 2a). This is in contrast to the charm-top-quark contribution where a tree-level matching at μ_W and μ_c is sufficient at LO.

After integrating out the charm quark the $\Delta S = 2$ effective Hamiltonian reads

$$\mathcal{H}_{f=3}^{\Delta S=2} = \frac{G_F^2}{4\pi^2} M_W^2 \left[\lambda_c^2 \eta_{cc} S(x_c) + \lambda_t^2 \eta_{tt} S(x_t) + 2\lambda_c \lambda_t \eta_{ct} S(x_c, x_t) \right] b(\mu) \tilde{Q}_{S2} + \text{h.c.} + \dots \quad (1.5)$$

where G_F is the Fermi constant and

$$\tilde{Q}_{S2} = (\bar{s}_L \gamma_\mu d_L) \otimes (\bar{s}_L \gamma^\mu d_L) \quad (1.6)$$

is the leading local four-quark operator that induces the $|\Delta S| = 2$ transition, defined in terms of the left-handed s - and d -quark fields. The QCD and logarithmic corrections are

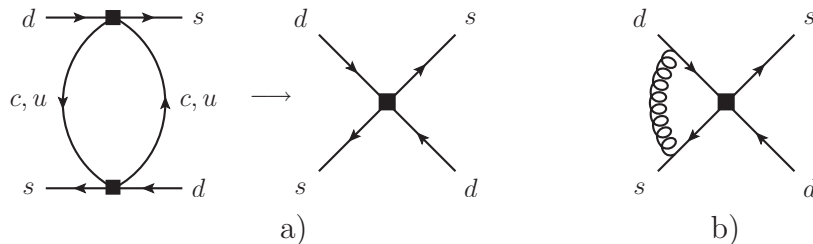


Figure 2: Dimension-six current-current and penguin operators mix at LO into \tilde{Q}_{S2} with a CKM factor $\lambda_t\lambda_c$ in a). Integrating out the charm quark results in similar diagrams for the LO and NLO matching of the contribution proportional to $\lambda_t\lambda_c$ and λ_c^2 , respectively. A sample diagram which is relevant to the LO evolution of \tilde{Q}_{S2} is shown in b).

known at LO [5] and NLO and are parametrised by $\eta_{cc} = 1.43(23)$ [6], $\eta_{ct} = 0.47(4)^1$ [7], and $\eta_{tt} = 0.5765(65)$ [8]. The parameter $b(\mu)$ is factored out such that

$$\hat{B}_K = \frac{3}{2}b(\mu) \frac{\langle \bar{K}^0 | \tilde{Q}_{S2} | K^0 \rangle}{f_K^2 M_K^2}, \quad (1.7)$$

where f_K is the Kaon decay constant, is a renormalisation-group invariant quantity, which can be calculated on the lattice with high precision – see for instance [9].

Finally note that $\mathcal{H}_{f=3}^{\Delta S=2}$ also contains higher-dimensional operators and current-current operators with up quarks, as indicated by the ellipses in Equation (1.5). At LO in the $1/N_c$ expansion (N_c being the number of colours) only one higher-dimensional operator is present and its matrix element is estimated in [3, 10] to result in a 0.5% enhancement of ϵ_K .

In view of the improvements on the long distance corrections achieved in the recent years, the short distance contributions should be reconsidered. In this work we calculate the NNLO corrections to the charm-top contribution η_{ct} . The NNLO corrections to the charm-quark contribution η_{cc} will be presented in a forthcoming publication [11].

This paper is organised as follows. In Section 2 we define the effective Hamiltonian relevant to $\Delta S = 2$ transitions. We present the details of our calculation as well as the analytic results in Section 3. The discussion and numerical evaluation follow in Section 4. In the appendix we show how our results transform under a change of the operator basis.

¹Our analysis, which uses different inputs for the physical parameters and a different error estimate, yields a NLO value of $\eta_{ct} = 0.455(69)$, see Section 4.

2 Effective Hamiltonian for Neutral Kaon Mixing

The effective Hamiltonian $\mathcal{H}_{f=3}^{\Delta S=2}$ of Equation (1.5) describes the dominant contribution to $\Delta S = 2$ processes below the charm-quark mass scale. The loop functions

$$S(x_c) = x_c + \mathcal{O}(x_c^2), \quad (2.1)$$

$$S(x_t) = \frac{4x_t - 11x_t^2 + x_t^3}{4(1-x_t)^2} - \frac{3x_t^3 \log x_t}{2(1-x_t)^3}, \quad (2.2)$$

$$S(x_c, x_t) = -x_c \log x_c + x_c F(x_t) + \mathcal{O}(x_c^2 \log x_c), \quad (2.3)$$

where the function F is defined as

$$F(x_t) = \frac{x_t^2 - 8x_t + 4}{4(1-x_t)^2} \log x_t - \frac{3x_t}{4(1-x_t)}, \quad (2.4)$$

are used as normalisation factors of the three contributions proportional to λ_c^2 , λ_t^2 , and $\lambda_c \lambda_t$ in Equation (1.5). In this normalisation we fix the charm-quark mass and the top-quark mass to $m_c = m_c^{\overline{MS}}(m_c)$ and $m_t = m_t^{\overline{MS}}(m_t)$ respectively in x_c and x_t . This avoids spurious scale dependences in η_{ct} , η_{cc} , and η_{tt} , if these parameters are defined through Equation (1.5).²

2.1 The Operator Basis

Above the charm-quark mass scale both the $\Delta S = 1$ and $\Delta S = 2$ effective Hamiltonian contributes to the Wilson coefficient of \tilde{Q}_{S2} through renormalisation group effects. In the following we list all operators needed for these effective Hamiltonians. They can be divided into three classes: Physical operators, gauge-invariant operators that vanish by the QCD equations of motion (EOM), and evanescent operators, that vanish algebraically in four space-time dimensions.

We start with the dimension-six operators, which we choose such that problems arising from the γ_5 matrix appearing in closed fermion loops in the framework of dimensional regularisation do not occur [12]. There are two current-current operators

$$\begin{aligned} Q_1^{qq'} &= (\bar{s}_L \gamma_\mu T^a q_L) \otimes (\bar{q}'_L \gamma^\mu T^a d_L), \\ Q_2^{qq'} &= (\bar{s}_L \gamma_\mu q_L) \otimes (\bar{q}'_L \gamma^\mu d_L), \end{aligned} \quad (2.5)$$

where $q_L = \frac{1}{2}(1 - \gamma_5)q$ is the left-handed chiral quark field, and q and q' are either u or c . The colour matrices T^a are normalised such that $\text{Tr } T^a T^b = \delta^{ab}/2$. We use these operators in the linear combination

$$Q_\pm^{qq'} = \frac{1}{2} \left(1 \pm \frac{1}{N_c} \right) Q_2^{qq'} \pm Q_1^{qq'} = \frac{1}{2} \left((\bar{s}_L^\alpha \gamma_\mu q_L^\alpha) \otimes (\bar{q}'_L^\beta \gamma^\mu d_L^\beta) \pm (\bar{s}_L^\alpha \gamma_\mu q_L^\beta) \otimes (\bar{q}'_L^\beta \gamma^\mu d_L^\alpha) \right), \quad (2.6)$$

²The parameters η_{cc} , η_{tt} , and η_{ct} equal η_1^* , η_2^* , and η_3^* , respectively, as defined in Reference [7].

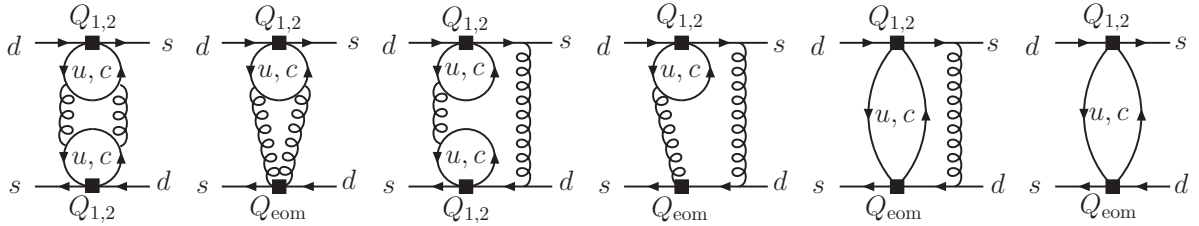


Figure 3: Sample three-loop diagrams with 1PI subdivergences that have to be subtracted by insertions of the EOM-vanishing operator. The corresponding 1PI one- and two-loop insertions of Q_{eom} are also shown.

where α and β are colour indices, and N_c is the number of colours. The advantage is that the anomalous dimensions in the subspace of current-current operators are diagonal in this basis³.

We define the QCD penguin operators as

$$\begin{aligned}
Q_3 &= (\bar{s}_L \gamma_\mu d_L) \otimes \sum_q (\bar{q} \gamma^\mu q), \\
Q_4 &= (\bar{s}_L \gamma_\mu T^a d_L) \otimes \sum_q (\bar{q} \gamma^\mu T^a q), \\
Q_5 &= (\bar{s}_L \gamma_{\mu_1 \mu_2 \mu_3} d_L) \otimes \sum_q (\bar{q} \gamma^{\mu_1 \mu_2 \mu_3} q), \\
Q_6 &= (\bar{s}_L \gamma_{\mu_1 \mu_2 \mu_3} T^a d_L) \otimes \sum_q (\bar{q} \gamma^{\mu_1 \mu_2 \mu_3} T^a q),
\end{aligned} \tag{2.7}$$

where the sum extends over the light quark fields, and we have introduced the abbreviations $\gamma_{\mu_1 \mu_2 \mu_3} = \gamma_{\mu_1} \gamma_{\mu_2} \gamma_{\mu_3}$, etc.

In order to subtract the divergences of all possible one-particle irreducible (1PI) sub-diagrams of the relevant Green's functions we need the following gauge-invariant EOM-vanishing operator

$$Q_{\text{eom}} = \frac{1}{g} \bar{s}_L \gamma^\mu T^a d_L D^\nu G_{\mu\nu}^a + Q_4, \tag{2.8}$$

where D_μ denotes the covariant derivative, acting on the gluon field, and $g^2 = 4\pi\alpha_s$ is the square of the strong coupling constant. Sample diagrams are shown in Figure 3.

The operator inducing the effective $|\Delta S| = 2$ interactions above the charm quark scale can be chosen as

$$\tilde{Q}_7 = \frac{m_c^2}{g^2 \mu^{2\epsilon}} (\bar{s}_L^\alpha \gamma_\mu d_L^\alpha) \otimes (\bar{s}_L^\beta \gamma^\mu d_L^\beta), \tag{2.9}$$

where α and β again denote colour indices: Note that, according to convention, we define the operator with two inverse powers of the strong coupling constant in order to account for the logarithm already present at leading order.

³This is true beyond LO only with a suitable choice of the evanescent operators, see below.

The use of dimensional regularisation in a theory involving fermions implies an infinite-dimensional Dirac algebra. In order to remove all divergences of the Green's functions, we have to introduce a set of evanescent operators that are non-zero in d dimensions and vanish algebraically in four dimensions. At the one-loop level we need

$$\begin{aligned}
E_1^{qq'(1)} &= (\bar{s}_L \gamma_{\mu_1 \mu_2 \mu_3} T^a q_L) \otimes (\bar{q}'_L \gamma^{\mu_1 \mu_2 \mu_3} T^a d_L) - (16 - 4\epsilon - 4\epsilon^2) Q_1^{qq'} , \\
E_2^{qq'(1)} &= (\bar{s}_L \gamma_{\mu_1 \mu_2 \mu_3} q_L) \otimes (\bar{q}'_L \gamma^{\mu_1 \mu_2 \mu_3} d_L) - (16 - 4\epsilon - 4\epsilon^2) Q_2^{qq'} , \\
E_3^{(1)} &= (\bar{s}_L \gamma_{\mu_1 \mu_2 \mu_3 \mu_4 \mu_5} d_L) \otimes \sum_q (\bar{q} \gamma^{\mu_1 \mu_2 \mu_3 \mu_4 \mu_5} q) + 64Q_3 - 20Q_5 , \\
E_4^{(1)} &= (\bar{s}_L \gamma_{\mu_1 \mu_2 \mu_3 \mu_4 \mu_5} T^a d_L) \otimes \sum_q (\bar{q} \gamma^{\mu_1 \mu_2 \mu_3 \mu_4 \mu_5} T^a q) + 64Q_4 - 20Q_6 .
\end{aligned} \tag{2.10}$$

At the two-loop level, we use the following four operators:

$$\begin{aligned}
E_1^{qq'(2)} &= (\bar{s}_L \gamma_{\mu_1 \mu_2 \mu_3 \mu_4 \mu_5} T^a q_L) \otimes (\bar{q}'_L \gamma^{\mu_1 \mu_2 \mu_3 \mu_4 \mu_5} T^a d_L) - \left(256 - 224\epsilon - \frac{5712}{25} \epsilon^2 \right) Q_1^{qq'} , \\
E_2^{qq'(2)} &= (\bar{s}_L \gamma_{\mu_1 \mu_2 \mu_3 \mu_4 \mu_5} q_L) \otimes (\bar{q}'_L \gamma^{\mu_1 \mu_2 \mu_3 \mu_4 \mu_5} d_L) - \left(256 - 224\epsilon - \frac{10032}{25} \epsilon^2 \right) Q_2^{qq'} , \\
E_3^{(2)} &= (\bar{s}_L \gamma_{\mu_1 \mu_2 \mu_3 \mu_4 \mu_5 \mu_6 \mu_7} d_L) \otimes \sum_q (\bar{q} \gamma^{\mu_1 \mu_2 \mu_3 \mu_4 \mu_5 \mu_6 \mu_7} q) + 1280Q_3 - 336Q_5 , \\
E_4^{(2)} &= (\bar{s}_L \gamma_{\mu_1 \mu_2 \mu_3 \mu_4 \mu_5 \mu_6 \mu_7} T^a d_L) \otimes \sum_q (\bar{q} \gamma^{\mu_1 \mu_2 \mu_3 \mu_4 \mu_5 \mu_6 \mu_7} T^a q) + 1280Q_4 - 336Q_6 .
\end{aligned} \tag{2.11}$$

The evanescent operators in the current-current sector are chosen such that the anomalous dimensions for the operators $Q_{\pm}^{qq'}$ are diagonal through NNLO [13]. The remaining operators are chosen as in Reference [12].

In addition to the operator \tilde{Q}_7 with the colour structure $(\bar{s}_L^\alpha \gamma_\mu d_L^\alpha) \otimes (\bar{s}_L^\beta \gamma^\mu d_L^\beta)$, the dimension-six and dimension-eight operators will also mix into an operator with the colour structure $(\bar{s}_L^\alpha \gamma_\mu d_L^\beta) \otimes (\bar{s}_L^\beta \gamma^\mu d_L^\alpha)$. In four space-time dimensions, the latter is related to the former structure by a Fierz transformation. The difference of these structures is therefore evanescent, and correspondingly we introduce an evanescent operator of the following form:

$$\tilde{E}_F = \frac{m_c^2}{g^2 \mu^{2\epsilon}} (\bar{s}_L^\alpha \gamma_\mu d_L^\beta) \otimes (\bar{s}_L^\beta \gamma^\mu d_L^\alpha) - \tilde{Q}_7 . \tag{2.12}$$

We choose the remaining evanescent dimension-eight operators to be

$$\begin{aligned}
\tilde{E}_7^{(1)} &= \frac{m_c^2}{g^2 \mu^{2\epsilon}} (\bar{s}_L^\alpha \gamma_{\mu_1 \mu_2 \mu_3} d_L^\alpha) \otimes (\bar{s}_L^\beta \gamma^{\mu_1 \mu_2 \mu_3} d_L^\beta) - (16 - 4\epsilon - 4\epsilon^2) \tilde{Q}_7, \\
\tilde{E}_8^{(1)} &= \frac{m_c^2}{g^2 \mu^{2\epsilon}} (\bar{s}_L^\alpha \gamma_{\mu_1 \mu_2 \mu_3} d_L^\beta) \otimes (\bar{s}_L^\beta \gamma^{\mu_1 \mu_2 \mu_3} d_L^\alpha) - (16 - 4\epsilon - 4\epsilon^2) (\tilde{Q}_7 + \tilde{E}_F), \\
\tilde{E}_7^{(2)} &= \frac{m_c^2}{g^2 \mu^{2\epsilon}} (\bar{s}_L^\alpha \gamma_{\mu_1 \mu_2 \mu_3 \mu_4 \mu_5} d_L^\alpha) \otimes (\bar{s}_L^\beta \gamma^{\mu_1 \mu_2 \mu_3 \mu_4 \mu_5} d_L^\beta) - (256 - 224\epsilon - \frac{108\,816}{325} \epsilon^2) \tilde{Q}_7, \\
\tilde{E}_8^{(2)} &= \frac{m_c^2}{g^2 \mu^{2\epsilon}} (\bar{s}_L^\alpha \gamma_{\mu_1 \mu_2 \mu_3 \mu_4 \mu_5} d_L^\beta) \otimes (\bar{s}_L^\beta \gamma^{\mu_1 \mu_2 \mu_3 \mu_4 \mu_5} d_L^\alpha) - (256 - 224\epsilon - \frac{108\,816}{325} \epsilon^2) (\tilde{Q}_7 + \tilde{E}_F), \\
\tilde{E}_7^{(3)} &= \frac{m_c^2}{g^2 \mu^{2\epsilon}} (\bar{s}_L^\alpha \gamma_{\mu_1 \mu_2 \mu_3 \mu_4 \mu_5 \mu_6 \mu_7} d_L^\alpha) \otimes (\bar{s}_L^\beta \gamma^{\mu_1 \mu_2 \mu_3 \mu_4 \mu_5 \mu_6 \mu_7} d_L^\beta) - 4096 \tilde{Q}_7, \\
\tilde{E}_8^{(3)} &= \frac{m_c^2}{g^2 \mu^{2\epsilon}} (\bar{s}_L^\alpha \gamma_{\mu_1 \mu_2 \mu_3 \mu_4 \mu_5 \mu_6 \mu_7} d_L^\beta) \otimes (\bar{s}_L^\beta \gamma^{\mu_1 \mu_2 \mu_3 \mu_4 \mu_5 \mu_6 \mu_7} d_L^\alpha) - 4096 (\tilde{Q}_7 + \tilde{E}_F).
\end{aligned} \tag{2.13}$$

This choice ensures that \tilde{Q}_{S2} will have the same anomalous dimension as Q_+ up to NNLO. It is given explicitly here for the first time.

2.2 Effective Hamiltonian

We obtain the effective Hamiltonian valid between the electroweak and the bottom-quark scale by removing the top quark and the W boson as dynamical degrees of freedom from the Standard Model. It reads in terms of the renormalised Wilson coefficients

$$\begin{aligned}
\mathcal{H}_{f=5}^{\text{eff}} &= \frac{4G_F}{\sqrt{2}} \sum_{i=+,-,3}^6 C_i \left[\sum_{j=+,-} Z_{ij} \sum_{k,l=u,c} V_{ks}^* V_{ld} Q_j^{kl} - \lambda_t \sum_{j=3}^6 Z_{ij} Q_j \right] \\
&+ \frac{G_F^2}{4\pi^2} \lambda_t^2 \tilde{C}_{S2}^t \tilde{Z}_{S2} \tilde{Q}_{S2} + 8G_F^2 \lambda_c \lambda_t \left[\sum_{k=+,-} \sum_{l=+,-,3}^6 C_k C_l \hat{Z}_{kl,7} + \tilde{C}_7 \tilde{Z}_{77} \right] \tilde{Q}_7 + \text{h.c.} .
\end{aligned} \tag{2.14}$$

Here the first line represents the $|\Delta S| = 1$ part of the effective Hamiltonian, whereas the second line contains the $|\Delta S| = 2$ contributions. The first term in the second line is related to a single insertion of \tilde{Q}_{S2} , induced by the top quark contribution to the Standard Model amplitude. The remaining terms arise from the mixing of insertions of two $|\Delta S| = 1$ operators into the operator \tilde{Q}_7 . The GIM mechanism leads to the absence of a λ_c^2 contribution to the Wilson coefficient of \tilde{Q}_7 . The renormalisation constants Z are defined such that any renormalised effective amplitude, of the form $\mathcal{A}_{\text{eff}} = C_i(\mu) Z_{ij} \langle Z Q_j \rangle_R + (C_k C_{k'} \hat{Z}_{kk',l} + \tilde{C}_k \tilde{Z}_{kl}) \langle Z \tilde{Q}_l \rangle_R$, is finite. Here angle-brackets denote matrix elements between initial and final states i and f , respectively, i.e. $\langle Q_j \rangle = \langle f | Q_j | i \rangle$. Z denotes the wave function renormalisation of the fields in the operator, so that $\langle Z Q_i \rangle_R$

are the renormalised matrix elements of the bare operator Q_i^{bare} , where masses and gauge couplings are renormalised in the usual way.

The effective Hamiltonian $\mathcal{H}_{f=4}^{\text{eff}}$ valid between the bottom- and the charm-quark scale looks exactly the same as $\mathcal{H}_{f=5}^{\text{eff}}$. The only difference is induced by the presence of penguin operators, which explicitly depend on all light quark fields.

Below the charm-quark scale, the charm quark is removed as a dynamical degree of freedom. As a consequence, the $|\Delta S| = 1$ operators can now be dropped from the effective Lagrangian, because the matrix elements of double insertions of these operators are suppressed by factors of m_s^2/M_W^2 . The effective Hamiltonian is thus given by

$$\mathcal{H}_{f=3}^{|\Delta S|=2} = \frac{G_F^2}{4\pi^2} \left[\lambda_c^2 \tilde{C}_{S2}^c(\mu) + \lambda_t^2 \tilde{C}_{S2}^t(\mu) + \lambda_c \lambda_t \tilde{C}_{S2}^{ct}(\mu) \right] \tilde{Z}_{S2} \tilde{Q}_{S2} \quad (2.15)$$

and now only contains the $|\Delta S| = 2$ operator \tilde{Q}_{S2} defined in Equation (1.6).

3 Calculation of η_{ct}

In this section we present the details of the calculation of η_{ct} in the NNLO approximation. We start with the determination of the initial conditions for the Wilson coefficients at the electroweak scale. Afterwards we use the renormalisation group equations to evolve them down to the charm-quark scale, including the threshold corrections at the bottom-quark scale. Finally we determine the charm-top contribution to \tilde{C}_{S2}^{ct} by a matching calculation at the charm-quark scale.

3.1 Initial Conditions at the Electroweak Scale

The initial conditions for the Wilson coefficients of the dimension-six operators are available in the literature. In our basis, where we can use a naive anticommuting γ_5 , the results up

to second order in $\alpha_s^{(f=5)}$ read⁴

$$\begin{aligned}
C_{\pm}(\mu) &= 1 \pm \frac{1}{2} \left(1 \mp \frac{1}{3} \right) (11 + 6 L_W) \frac{\alpha_s^{(5)}(\mu)}{4\pi} + \left(\frac{1}{18} (7 \pm 51) \pi^2 \mp \frac{1}{2} \left(1 \mp \frac{1}{3} \right) T(x_t) \right. \\
&\quad \left. - \frac{1}{3600} (135677 \mp 124095) - \frac{5}{36} (11 \mp 249) L_W + \frac{1}{6} (7 \pm 51) L_W^2 \right) \left(\frac{\alpha_s^{(5)}(\mu)}{4\pi} \right)^2, \\
C_3(\mu) &= \left(\frac{\alpha_s^{(5)}(\mu)}{4\pi} \right)^2 \left(G_1^t(x_t) - \frac{680}{243} - \frac{20}{81} \pi^2 - \frac{68}{81} L_W - \frac{20}{27} L_W^2 \right), \\
C_4(\mu) &= \frac{\alpha_s^{(5)}(\mu)}{4\pi} \left(E_0^t(x_t) - \frac{7}{9} + \frac{2}{3} L_W \right) \\
&\quad + \left(\frac{\alpha_s^{(5)}(\mu)}{4\pi} \right)^2 \left(E_1^t(x_t) + \frac{842}{243} + \frac{10}{81} \pi^2 + \frac{124}{27} L_W + \frac{10}{27} L_W^2 \right), \\
C_5(\mu) &= \left(\frac{\alpha_s^{(5)}(\mu)}{4\pi} \right)^2 \left(\frac{2}{15} E_0^t(x_t) - \frac{1}{10} G_1^t(x_t) + \frac{68}{243} + \frac{2}{81} \pi^2 + \frac{14}{81} L_W + \frac{2}{27} L_W^2 \right), \\
C_6(\mu) &= \left(\frac{\alpha_s^{(5)}(\mu)}{4\pi} \right)^2 \left(\frac{1}{4} E_0^t(x_t) - \frac{3}{16} G_1^t(x_t) + \frac{85}{162} + \frac{5}{108} \pi^2 + \frac{35}{108} L_W + \frac{5}{36} L_W^2 \right).
\end{aligned} \tag{3.1}$$

We have taken the initial conditions for C_{\pm} from Reference [13]. The initial conditions for $C_3 \dots C_6$ can be found in Reference [14], where also the loop functions $T(x_t)$, $G_1^t(x_t)$, $E_0^t(x_t)$ and $E_1^t(x_t)$ are defined. Note that in our renormalisation scheme we had to include an additional finite contribution for C_4 , as described in the appendix. We have introduced the abbreviation $L_W = \log(\mu^2/M_W^2)$.

With these ingredients, we can now calculate the initial conditions for the Wilson coefficients of the dimension-eight operators. In order to match the Green's functions in the Standard Model and the effective five-flavour theory, we have to compute the finite parts of Feynman diagrams of the type shown in Figures 1 and 4. To this end, we perform a Taylor expansion in the charm-quark mass of all propagators corresponding to a charm-quark field. The constant terms cancel because of the GIM mechanism, whereas the terms proportional to m_c^2 give the leading non-vanishing contribution we are interested in. This procedure leads to massless vacuum integrals in the effective theory, such that only terms proportional to tree-level matrix elements remain. Some of these terms multiply divergent renormalisation constants and correspond to infrared divergences in the effective theory. They exactly cancel the corresponding infrared divergent terms in the Standard Model, leaving us with a finite result.

⁴Here and in the following, by the superscript in brackets we display explicitly the number of light quark flavours for which α_s is defined.

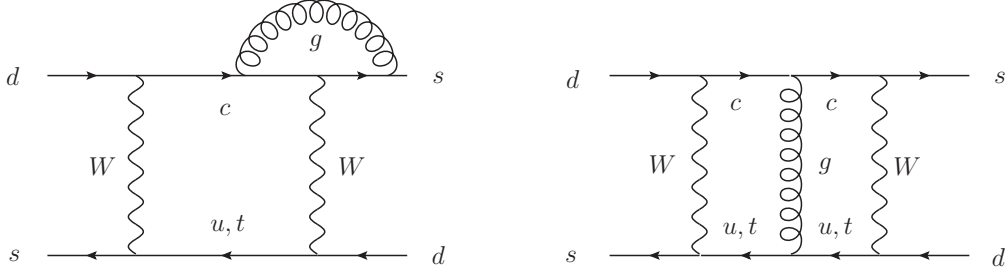


Figure 4: Sample two-loop Feynman diagrams contributing to the matching at the electroweak scale.

Expanding the dimension-eight Wilson coefficient as

$$\tilde{C}_7(\mu) = \tilde{C}_7^{(0)}(\mu) + \frac{\alpha_s^{(5)}(\mu)}{4\pi} \tilde{C}_7^{(1)}(\mu) + \left(\frac{\alpha_s^{(5)}(\mu)}{4\pi} \right)^2 \tilde{C}_7^{(2)}(\mu), \quad (3.2)$$

we obtain the following result:

$$\begin{aligned} \tilde{C}_7^{(0)}(\mu) &= 0, & \tilde{C}_7^{(1)}(\mu) &= F(x_t) + \frac{1}{2} - L_W, \\ \tilde{C}_7^{(2)}(\mu) &= + \frac{5x_t^3 - 21x_t^2 + 60x_t - 20}{2(x_t - 1)^3} \log(x_t) L_W \\ &+ \frac{12x_t^5 - 34x_t^4 - 9x_t^3 - 33x_t^2 - 116x_t + 36}{12(x_t - 1)^3} \log^2(x_t) \\ &+ \frac{-12x_t^5 + 27x_t^4 + 23x_t^3 + 150x_t^2 - 108x_t + 16}{6(x_t - 1)^3 x_t} \log(x_t) \\ &+ \frac{-7800x_t^4 - 126499x_t^3 + 191248x_t^2 - 129749x_t + 10400}{3900(x_t - 1)^2 x_t} \\ &+ \frac{6x_t^6 - 11x_t^5 - 8x_t^4 - 29x_t^3 + 23x_t^2 - 16x_t + 8}{3(x_t - 1)^2 x_t^2} \text{Li}_2(1 - x_t) \\ &+ \frac{6x_t^4 + x_t^3 - 59x_t^2 - 8}{3x_t^2} \zeta_2 - \frac{47x_t^2 - 31x_t + 56}{6(x_t - 1)^2} L_W - 7L_W^2 \end{aligned} \quad (3.3)$$

The first line in Equation (3.3) agrees with the result obtained already by Herrlich and Nierste in [7] after the corresponding change of the renormalisation scheme. The two-loop result is new.

3.2 Structure of the Renormalisation Group Equations

After the determination of the initial conditions for the Wilson coefficients, the next step is the renormalisation group evolution to lower scales. The renormalisation group equation

relevant for the Wilson coefficient \tilde{C}_7 is given by:

$$\mu \frac{d}{d\mu} \tilde{C}_7(\mu) = \tilde{C}_7(\mu) \tilde{\gamma}_{77} + \sum_{k=+,-} \sum_{n=+,-,3}^6 C_k(\mu) C_n(\mu) \hat{\gamma}_{kn,7}, \quad (3.4)$$

where $\tilde{\gamma}_{77}$ denotes the anomalous dimension matrix of the operator \tilde{Q}_7 , and $\hat{\gamma}_{kn,7}$ is the anomalous dimension tensor, describing the mixing of the dimension-six operators into \tilde{Q}_7 . The matrix $\tilde{\gamma}_{77}$ is decomposed as $\tilde{\gamma}_{77} = \tilde{\gamma}_{S2} + 2\gamma_m - 2\beta$, where the anomalous dimension of the quark mass γ_m and the β function are related to the factor m_c^2/g^2 in the definition of the operator \tilde{Q}_7 . The anomalous dimension matrix $\tilde{\gamma}_{S2}$ is defined in terms of the renormalisation constants \tilde{Z}_{S2} as

$$\tilde{\gamma}_{S2} = \tilde{Z}_{S2} \mu \frac{d}{d\mu} \tilde{Z}_{S2}^{-1}. \quad (3.5)$$

The explicit expressions for the anomalous dimension matrix in terms of the renormalisation constants \tilde{Z}_{S2} are given up to NNLO by

$$\begin{aligned} \tilde{\gamma}_{S2}^{(0)} &= 2\tilde{Z}_{S2}^{(1,1)}, & \tilde{\gamma}_{S2}^{(1)} &= 4\tilde{Z}_{S2}^{(2,1)} - 2\tilde{Z}_{S2}^{(1,1)} \tilde{Z}_{S2}^{(1,0)}, \\ \tilde{\gamma}_{S2}^{(2)} &= 6\tilde{Z}_{S2}^{(3,1)} - 4\tilde{Z}_{S2}^{(2,1)} \tilde{Z}_{S2}^{(1,0)} - 2\tilde{Z}_{S2}^{(1,1)} \tilde{Z}_{S2}^{(2,0)}, \end{aligned} \quad (3.6)$$

where we only kept the non-vanishing physical contributions. Here the superscript (n, m) denotes the $1/\epsilon^m$ -pole part of the n -loop contribution. The anomalous dimension tensor is defined as [15]

$$\hat{\gamma}_{kn,l} = -(\gamma_{kk'} \delta_{nn'} + \gamma_{nn'} \delta_{kk'}) \hat{Z}_{k'n',l} \tilde{Z}_{l'l}^{-1} - \left(\mu \frac{d}{d\mu} \hat{Z}_{kn,l} \right) \tilde{Z}_{l'l}^{-1}. \quad (3.7)$$

The non-vanishing contributions to the physical part of the anomalous dimension tensor are given in terms of the renormalisation constants by

$$\begin{aligned} \hat{\gamma}_{kn,l}^{(0)} &= 2\hat{Z}_{kn,l}^{(1,1)}, \\ \hat{\gamma}_{kn,l}^{(1)} &= 4\hat{Z}_{kn,l}^{(2,1)} - 2\hat{Z}_{kn,l'}^{(1,1)} \tilde{Z}_{l'l}^{(1,0)} - 2 \left\{ Z_{kk'}^{(1,1)} \delta_{nn'} + \delta_{kk'} Z_{nn'}^{(1,1)} \right\} \hat{Z}_{k'n',l}^{(1,0)}, \\ \hat{\gamma}_{kn,l}^{(2)} &= 6\hat{Z}_{kn,l}^{(3,1)} - 4\hat{Z}_{kn,l'}^{(2,1)} \tilde{Z}_{l'l}^{(1,0)} - 2\hat{Z}_{kn,l'}^{(1,1)} \tilde{Z}_{l'l}^{(2,0)} \\ &\quad - 2 \left\{ Z_{kk'}^{(1,1)} \delta_{nn'} + \delta_{kk'} Z_{nn'}^{(1,1)} \right\} \hat{Z}_{k'n',l}^{(2,0)} - 4 \left\{ Z_{kk'}^{(2,1)} \delta_{nn'} + \delta_{kk'} Z_{nn'}^{(2,1)} \right\} \hat{Z}_{k'n',l}^{(1,0)}, \end{aligned} \quad (3.8)$$

where the indices k , n and l correspond to physical operators only.

In order to determine the renormalisation constants, we have to compute the divergent parts of Feynman diagrams with up to three loops, see Figure 5. We use the method suggested in [16] by Chetyrkin, Misiak and Münz for extracting the UV divergences of a given Feynman diagram. The renormalisation constants are then determined recursively

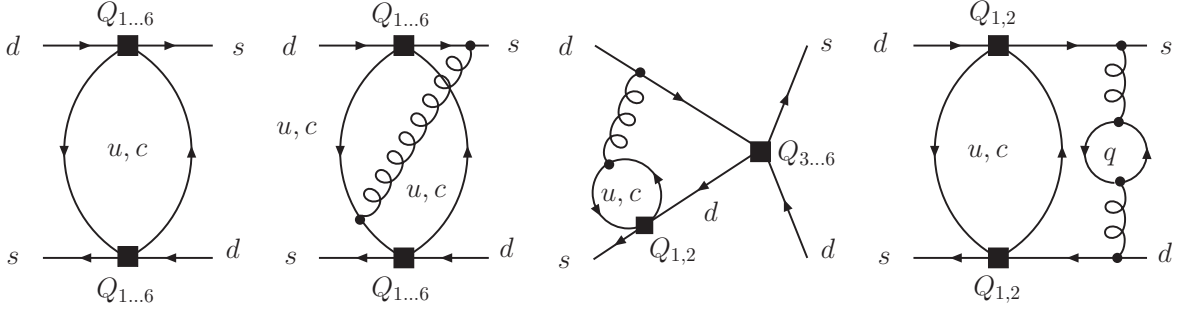


Figure 5: Sample one-, two-, and three-loop diagrams contributing to the NNLO mixing of dimension-six into dimension-eight operators.

by subtracting subdivergences according to Zimmermann's forest formula. As usual, we perform a finite renormalisation in order to ensure the vanishing of matrix elements of evanescent operators. An additional subtlety arises because of the presence of EOM-vanishing operators at second order in the effective interactions: As explained in detail in Reference [17], we have to expect non-trivial contact terms resulting from double insertions of Q_{eom} and physical operators. We computed these terms explicitly, showing that non-zero contributions indeed occur, and subtracted them by an additional finite counterterm:

$$\hat{Z}_{Q+Q_{\text{eom}},\tilde{Q}_7}^{(2,0)} = \hat{Z}_{Q-Q_{\text{eom}},\tilde{Q}_7}^{(2,0)} = \frac{3}{8} \left(N_c - 1 - \frac{1}{N_c} - \frac{1}{N_c^2} \right). \quad (3.9)$$

This renormalisation ensures the validity of the equations of motion also at second order in the effective interactions.

Let us now look at the equations (3.4) in more detail. It turns out that these equations are equivalent to the following system of eight equations [7]

$$\mu \frac{d}{d\mu} D = \gamma^T D, \quad (3.10)$$

where the anomalous dimension matrix and the Wilson coefficients are now given by

$$\gamma^T = \begin{pmatrix} \gamma_Q^T & 0 & 0 \\ \tilde{\gamma}_{+,7}^T & \tilde{\gamma}_{77} - \gamma_+ & 0 \\ \tilde{\gamma}_{-,7}^T & 0 & \tilde{\gamma}_{77} - \gamma_- \end{pmatrix}, \quad D(\mu) = \begin{pmatrix} C(\mu) \\ \tilde{C}_7^+(\mu)/C_+(\mu) \\ \tilde{C}_7^-(\mu)/C_-(\mu) \end{pmatrix}, \quad (3.11)$$

if we decompose the Wilson coefficient \tilde{C}_7 as

$$\tilde{C}_7(\mu) = \tilde{C}_7^+(\mu) + \tilde{C}_7^-(\mu). \quad (3.12)$$

This decomposition is completely arbitrary and preserved by the renormalisation group evolution. For instance, we may choose $\tilde{C}_7^+(\mu) = \tilde{C}_7(\mu)$ and $\tilde{C}_7^-(\mu) = 0$. The advantage of (3.10) is that it has the form of a renormalisation group equation for a single operator insertion, and we can use the well known explicit solution (see, for instance, Reference [4]).

We obtain the anomalous dimension matrix γ_Q of the operators $Q_+, Q_-, Q_3, \dots, Q_6$ from Reference [4] by the basis transformation described in the appendix and find

$$\gamma_Q^{(0)} = \begin{pmatrix} 4 & 0 & 0 & \frac{2}{3} & 0 & 0 \\ 0 & -8 & 0 & \frac{2}{3} & 0 & 0 \\ 0 & 0 & 0 & -\frac{52}{3} & 0 & 2 \\ 0 & 0 & -\frac{40}{9} & \frac{4}{3}f - \frac{160}{9} & \frac{4}{9} & \frac{5}{6} \\ 0 & 0 & 0 & -\frac{256}{3} & 0 & 20 \\ 0 & 0 & -\frac{256}{9} & \frac{40}{3}f - \frac{544}{9} & \frac{40}{9} & -\frac{2}{3} \end{pmatrix}, \quad (3.13)$$

$$\gamma_Q^{(1)} = \begin{pmatrix} \frac{4}{9}f-7 & 0 & -\frac{748}{81} & \frac{415}{81} & \frac{82}{81} & \frac{35}{54} \\ 0 & -\frac{8}{9}f-14 & \frac{332}{81} & \frac{793}{81} & -\frac{26}{81} & \frac{35}{54} \\ 0 & 0 & -\frac{4468}{81} & -\frac{52}{9}f - \frac{29129}{81} & \frac{400}{81} & \frac{3493}{108} - \frac{2}{9}f \\ 0 & 0 & \frac{368}{81}f - \frac{13678}{243} & \frac{1334}{81}f - \frac{79409}{243} & \frac{509}{486} - \frac{8}{81}f & \frac{13499}{648} - \frac{5}{27}f \\ 0 & 0 & -\frac{160}{9}f - \frac{244480}{81} & -\frac{2200}{9}f - \frac{29648}{81} & \frac{16Nf}{9} + \frac{23116}{81} & \frac{148}{9}f + \frac{3886}{27} \\ 0 & 0 & \frac{77600}{243} - \frac{1264}{81}f & \frac{164}{81}f - \frac{28808}{243} & \frac{400}{81}f - \frac{20324}{243} & \frac{622}{27}f - \frac{21211}{162} \end{pmatrix}, \quad (3.14)$$

$$\gamma_Q^{(2)} = \begin{pmatrix} \frac{275267}{150} - \frac{260}{81}f^2 - \frac{52891}{675}f - \left(\frac{160}{3}f + 672\right)\zeta_3 & 0 \\ 0 & \frac{12297}{25} + \frac{520}{81}f^2 - \frac{62686}{675}f + \left(\frac{320}{3}f + 672\right)\zeta_3 \\ 0 & 0 \\ 0 & 0 \\ 0 & 0 \\ 0 & 0 \end{pmatrix} \cdot \begin{pmatrix} \frac{54821}{4374} - \frac{160}{243}f + \frac{1360}{27}\zeta_3 & -\frac{8226427}{109350} - \frac{18845}{1458}f - \frac{2104}{27}\zeta_3 \\ \frac{1064}{243}f + \frac{1360}{27}\zeta_3 - \frac{25531}{4374} & -\frac{26513}{1458}f - \frac{664}{27}\zeta_3 + \frac{57546991}{218700} \\ \frac{14012}{243}f - \frac{608}{27}\zeta_3 - \frac{4203068}{2187} & \frac{272}{27}f^2 + \frac{888605}{2916}f + \left(160f + \frac{39824}{27}\right)\zeta_3 - \frac{18422762}{2187} \\ \frac{472}{81}f^2 + \frac{217892}{2187}f + \left(\frac{1360}{9}f + \frac{27520}{81}\right)\zeta_3 - \frac{5875184}{6561} & -\frac{4010}{729}f^2 + \frac{8860733}{17496}f + \left(\frac{2512}{27}f + \frac{16592}{81}\right)\zeta_3 - \frac{70274587}{13122} \\ -\frac{2144}{81}f^2 + \frac{358672}{81}f + \frac{87040}{27}\zeta_3 - \frac{194951552}{2187} & \frac{3088}{27}f - \frac{2949616}{729}f + \left(640f + \frac{238016}{27}\right)\zeta_3 - \frac{130500332}{2187} \\ \frac{17920}{243}f^2 - \frac{2535466}{2187}f + \left(\frac{12160}{9}f + \frac{174208}{81}\right)\zeta_3 + \frac{162733912}{6561} & -\frac{159548}{729}f^2 - \frac{1826023}{4374}f - \left(\frac{9440}{27}f + \frac{24832}{81}\right)\zeta_3 + \frac{13286236}{6561} \end{pmatrix} \cdot \begin{pmatrix} \frac{112}{243}f - \frac{124}{27}\zeta_3 - \frac{113417}{17496} & -\frac{35}{324}f - \frac{40}{9}\zeta_3 + \frac{479581}{23328} \\ -\frac{140}{243}f - \frac{124}{27}\zeta_3 + \frac{79687}{17496} & -\frac{35}{324}f - \frac{70}{9}\zeta_3 + \frac{242737}{23328} \\ -\frac{1352}{243}f - \frac{496}{27}\zeta_3 + \frac{674281}{4374} & \frac{9284531}{11664} - \frac{26}{27}f^2 - \frac{2798}{81}f - \left(20f + \frac{1921}{9}\right)\zeta_3 \\ -\frac{52}{81}f^2 - \frac{31175}{8748}f - \left(\frac{136f}{9} + \frac{3154}{81}\right)\zeta_3 + \frac{2951809}{52488} & \frac{3227801}{8748} - \frac{65}{54}f^2 - \frac{105293}{11664}f + \left(\frac{200}{27} - \frac{220}{9}f\right)\zeta_3 \\ \frac{272}{81}f^2 - \frac{27428}{81}f - \frac{13984}{27}\zeta_3 + \frac{14732222}{2187} & \frac{16521659}{2916} - \frac{316}{27}f^2 + \frac{8081}{54}f - \left(200f + \frac{22420}{9}\right)\zeta_3 \\ -\frac{1720}{243}f^2 + \frac{395783}{4374}f + \left(-\frac{1360}{9}f - \frac{33832}{81}\right)\zeta_3 - \frac{22191107}{13122} & -\frac{533}{81}f^2 + \frac{3353393}{5832}f + \left(\frac{9248}{27} - \frac{1120}{9}f\right)\zeta_3 - \frac{32043361}{8748} \end{pmatrix}. \quad (3.15)$$

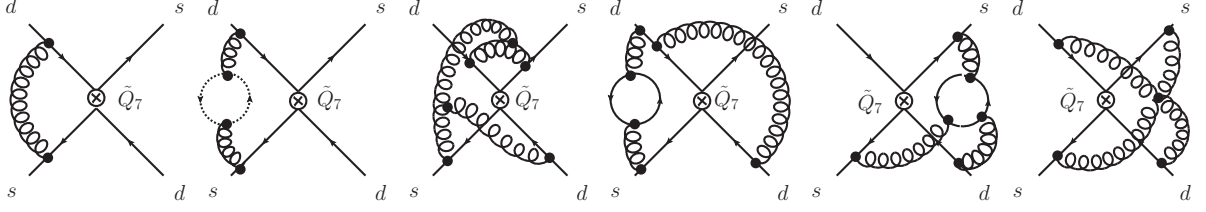


Figure 6: Sample one-, two-, and three-loop diagrams, whose divergent parts contribute to the anomalous dimensions of the operator \tilde{Q}_7 . Curly lines denote gluons, dotted lines denote ghosts, and solid lines denote quarks.

Here and in the following, f is the number of active quark flavours.

We denote the anomalous dimension for the double insertion of either Q_+ or Q_- and one of the operators $Q_+, Q_-, Q_3, \dots, Q_6$ by

$$\tilde{\gamma}_{\pm,7}^T = (\tilde{\gamma}_{\pm+,7}, \tilde{\gamma}_{\pm-,7}, \tilde{\gamma}_{\pm 3,7}, \tilde{\gamma}_{\pm 4,7}, \tilde{\gamma}_{\pm 5,7}, \tilde{\gamma}_{\pm 6,7}), \quad (3.16)$$

and find

$$\tilde{\gamma}_{+,7}^{T(0)} = (-3, 1, 0, 0, -96, -8), \quad \tilde{\gamma}_{-,7}^{T(0)} = (1, -1, 0, 0, 48, -8), \quad (3.17)$$

$$\tilde{\gamma}_{+,7}^{T(1)} = \left(-30, 23, -\frac{140}{3}, -\frac{341}{9}, -\frac{248}{3}, \frac{1252}{9} \right), \quad (3.18)$$

$$\tilde{\gamma}_{-,7}^{T(1)} = \left(23, -46, \frac{4}{3}, -\frac{101}{9}, -\frac{680}{3}, -\frac{164}{9} \right),$$

$$\tilde{\gamma}_{+,7}^{T(2)} = \left(\frac{5437543}{2808} - \frac{158279}{1950}f + 252\zeta_3, \frac{166441}{5850}f + \frac{106\zeta_3}{3} - \frac{8107577}{7020}, \right. \\ \left. \frac{40}{9}f - \frac{472}{3}\zeta_3 + \frac{27909247}{7020}, \frac{578}{27}f - \frac{2698}{9}\zeta_3 + \frac{5333399}{3240}, \right. \\ \left. \frac{225176}{195}f + \frac{6128}{3}\zeta_3 - \frac{9973214}{1755}, \frac{4712717}{1755}f + \frac{4856}{9}\zeta_3 - \frac{832816243}{10530} \right), \quad (3.19)$$

$$\tilde{\gamma}_{-,7}^{T(2)} = \left(\frac{166441}{5850}f + \frac{106}{3}\zeta_3 - \frac{8107577}{7020}, \frac{93707}{5850}f + \frac{104}{3}\zeta_3 - \frac{23496713}{70200}, \right. \\ \left. -\frac{32}{9}f + \frac{200}{3}\zeta_3 - \frac{30781813}{35100}, -\frac{94}{27}f - \frac{922}{9}\zeta_3 - \frac{31831601}{210600}, \right. \\ \left. \frac{364552}{975}f + \frac{1328}{3}\zeta_3 - \frac{83770148}{1755}, \frac{1412938999}{52650} - \frac{6223223}{8775}f + \frac{4328}{9}\zeta_3 \right),$$

at LO, NLO, and NNLO, respectively. The LO and NLO results agree with the literature [7] after the corresponding change of the operator basis, described in the appendix. The NNLO result is new.

We have chosen the evanescent operators in the dimension-eight sector in such a way that the anomalous dimension of the operator \tilde{Q}_{S2} equals the anomalous dimension of Q_+

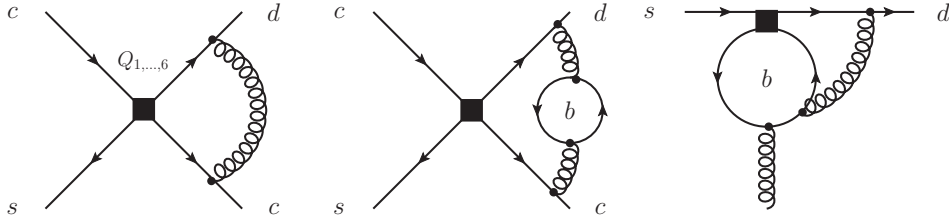


Figure 7: Feynman diagrams relevant for the threshold corrections at the bottom quark scale. The one-loop diagram of Q_1 and Q_2 is the same in both theories, whereas at the two-loop level they receive non-trivial corrections from virtual bottom quarks. The same applies to insertions of the operator \tilde{Q}_7 . Because the penguin operators mix into Q_{com} , we also had to calculate insertions of $Q_{3,\dots,6}$ with one external gluon, expanding up to the second power in the external momenta.

through NNLO. Consequently $\tilde{\gamma}_{S2} = \gamma_+$, and [13]

$$\begin{aligned} \gamma_+^{(0)} &= 4, & \gamma_+^{(1)} &= \frac{4}{9}f - 7, \\ \gamma_+^{(2)} &= \frac{275\,267}{150} - \frac{52\,891}{675}f - \frac{260}{81}f^2 - \left(\frac{160}{3}f + 672\right)\zeta_3. \end{aligned} \quad (3.20)$$

The explicit expressions for the QCD β function and the anomalous dimension of the quark mass are given by [18–21]:

$$\beta_0 = 11 - \frac{2}{3}f, \quad \beta_1 = 102 - \frac{38}{3}f, \quad \beta_2 = \frac{2857}{2} - \frac{5033}{18}f + \frac{325}{54}f^2, \quad (3.21)$$

and

$$\gamma_m^{(0)} = 8, \quad \gamma_m^{(1)} = \frac{404}{3} - \frac{40}{9}f, \quad \gamma_m^{(2)} = 2498 - \left(\frac{4432}{27} + \frac{320}{3}\zeta_3\right)f - \frac{280}{81}f^2. \quad (3.22)$$

3.3 Threshold Corrections at the Bottom-Quark Scale

When we pass the bottom-quark threshold, we must perform a proper matching between the effective theories with five and four flavours. This threshold correction is computed by requiring the equality of the Green's functions in the two theories at the matching scale, in this case $\mu_b = \mathcal{O}(m_b)$, where m_b is the bottom-quark mass.

At NNLO, there are several sources of matching corrections. The penguin operators are affected already at NLO, because they explicitly depend on the number of light-quark fields. At NNLO also the matching of the current-current and the dimension-eight operators is non-trivial. The source of such contributions are virtual bottom quarks in two-loop matrix elements of the form shown in Figure 7. In addition, also the strong coupling constant and the charm-quark mass are discontinuous beyond LO.

Let us write the equality of a general amplitude in the two theories at the matching scale μ_f as

$$C_{f-1}(\mu_f)\langle Q_{f-1}\rangle(\mu_f) = C_f(\mu_f)\langle Q_f\rangle(\mu_f), \quad (3.23)$$

the variables with subscripts f and $f - 1$ belonging to the f - and $f - 1$ -flavour theory. At the bottom-quark scale, we have $f = 5$. We parameterise the matrix elements of the operators as an expansion in the coupling constant defined in the corresponding f -flavour theory:

$$\langle Q_f \rangle(\mu_f) = \left(1 + \frac{\alpha_s^{(f)}(\mu_f)}{4\pi} r_f^{(1)}(\mu_f) + \left(\frac{\alpha_s^{(f)}(\mu_f)}{4\pi} \right)^2 r_f^{(2)}(\mu_f) \right) \langle Q_f \rangle^{(0)}. \quad (3.24)$$

An additional subtlety arises, because the strong coupling constant also gets a non-trivial matching correction at a flavour threshold. Up to the NNLO approximation we have the relation [22–24]

$$\begin{aligned} \alpha_s^{(f)}(\mu_f) = & \alpha_s^{(f-1)}(\mu_f) \left(1 + \frac{\alpha_s^{(f-1)}(\mu_f)}{4\pi} \frac{2}{3} \log \frac{\mu_f^2}{m_f^2} \right. \\ & \left. - \left(\frac{\alpha_s^{(f-1)}(\mu_f)}{4\pi} \right)^2 \left(\frac{22}{9} - \frac{22}{3} \log \frac{\mu_f^2}{m_f^2} - \frac{4}{9} \log^2 \frac{\mu_f^2}{m_f^2} \right) \right), \end{aligned} \quad (3.25)$$

which we use to express all quantities in terms of the coupling constant $\alpha_s^{(f-1)}(\mu_f)$ in the effective theory with $f - 1$ flavours. Here $m_f = m_f(\mu_f)$ is the $\overline{\text{MS}}$ mass of the quark which is integrated out. Note that the matching for \tilde{C}_7 starts at order $1/\alpha_s$, so that by inverting Equation (3.25) we get a contribution already at NLO. Similarly, we need the decoupling relation for the charm quark mass up to NNLO [25]:

$$m_c^{(f-1)}(\mu_f) = m_c^{(f)}(\mu_f) \left[1 + \left(\frac{\alpha_s^{(f)}(\mu_f)}{4\pi} \right)^2 \left(\frac{89}{27} - \frac{20}{9} \log \frac{\mu_f^2}{m_f^2} + \frac{4}{3} \log^2 \frac{\mu_f^2}{m_f^2} \right) \right]. \quad (3.26)$$

In order to display the threshold corrections explicitly, we now introduce the discontinuities

$$\delta C^{(k)}(\mu_f) = C_f^{(k)}(\mu_f) - C_{f-1}^{(k)}(\mu_f), \quad \delta r^{(k)}(\mu_f) = r_f^{(k)}(\mu_f) - r_{f-1}^{(k)}(\mu_f), \quad (3.27)$$

of the Wilson coefficients and the matrix elements, respectively, and find for the general solution of Equation (3.23), in case of the dimension-six Wilson coefficients:

$$\begin{aligned} \delta C^{(0)}(\mu_f) = & 0, \quad \delta C^{(1)}(\mu_f) = -C_f^{(0)}(\mu_f) \delta r^{(1)}(\mu_f), \\ \delta C^{(2)}(\mu_f) = & -C_f^{(1)}(\mu_f) \left(\delta r^{(1)}(\mu_f) + \frac{2}{3} \log \frac{\mu_f^2}{m_f^2} \right) \\ & - C_f^{(0)}(\mu_f) \left(\delta r^{(2)}(\mu_f) - \delta r^{(1)}(\mu_f) r_{f-1}^{(1)}(\mu_f) + \frac{2}{3} r_f^{(1)}(\mu_f) \log \frac{\mu_f^2}{m_f^2} \right). \end{aligned} \quad (3.28)$$

Notice that the different single contributions in the last bracket may not be finite because of spurious IR divergences, which nevertheless cancel in the sum. The matching corrections

look different for the dimension-eight Wilson coefficients, because of the factor $1/g^2$ in front of the operator:

$$\begin{aligned}\delta\tilde{C}^{(0)}(\mu_f) &= 0, & \delta\tilde{C}^{(1)}(\mu_f) &= -\tilde{C}_f^{(0)}(\mu_f) \left(\delta\tilde{r}^{(1)}(\mu_f) - \frac{2}{3} \log \frac{\mu_f^2}{m_f^2} \right), \\ \delta\tilde{C}^{(2)}(\mu_f) &= -\tilde{C}_f^{(1)}(\mu_f) \delta\tilde{r}^{(1)}(\mu_f) - \tilde{C}_f^{(0)}(\mu_f) \left[\delta\tilde{r}^{(2)}(\mu_f) \right. \\ &\quad \left. - \left(\delta\tilde{r}^{(1)}(\mu_f) - \frac{2}{3} \log \frac{\mu_f^2}{m_f^2} \right) \tilde{r}_{f-1}^{(1)}(\mu_f) + \frac{22}{9} - \frac{22}{3} \log \frac{\mu_f^2}{m_f^2} \right].\end{aligned}\tag{3.29}$$

In addition, we have to take into account the terms related to the decoupling of the charm-quark mass.

At NLO, only the matrix elements of the penguin operators get non-vanishing contributions. They can be obtained from

$$\delta r_Q^{(1)}(\mu_b) = \begin{pmatrix} 0 & 0 & 0 & 0 & 0 & 0 \\ 0 & 0 & 0 & 0 & 0 & 0 \\ 0 & 0 & 0 & 0 & 0 & 0 \\ 0 & 0 & 0 & -\frac{2}{3} \log \frac{\mu_b^2}{m_b^2} & 0 & 0 \\ 0 & 0 & 0 & 0 & 0 & 0 \\ 0 & 0 & 0 & 4 - \frac{20}{3} \log \frac{\mu_b^2}{m_b^2} & 0 & 0 \end{pmatrix},\tag{3.30}$$

where δr_Q denotes the difference of the matrix elements in the subspace of dimension-six operators. At NNLO, we obtain the following contributions for the penguin operators:

$$\delta r_Q^{(2)}(\mu_b) - \delta r_Q^{(1)}(\mu_b) r_{Q,f=4}^{(1)}(\mu_b) + \frac{2}{3} r_{Q,f=5}^{(1)}(\mu_b) \log \frac{\mu_b^2}{m_b^2} = \begin{pmatrix} a_+^{(2)} & 0 & 0 & 0 & 0 & 0 \\ 0 & a_-^{(2)} & 0 & 0 & 0 & 0 \\ 0 & 0 & a_{33}^{(2)} & a_{34}^{(2)} & a_{35}^{(2)} & a_{36}^{(2)} \\ 0 & 0 & a_{43}^{(2)} & a_{44}^{(2)} & a_{45}^{(2)} & a_{46}^{(2)} \\ 0 & 0 & a_{53}^{(2)} & a_{54}^{(2)} & a_{55}^{(2)} & a_{56}^{(2)} \\ 0 & 0 & a_{63}^{(2)} & a_{64}^{(2)} & a_{65}^{(2)} & a_{66}^{(2)} \end{pmatrix},\tag{3.31}$$

where we can extract $a_+^{(2)}$ and $a_-^{(2)}$ from [13] to find

$$a_{\pm}^{(2)} = \delta r_{\pm}^{(2)}(\mu_b) = \mp \left(1 \mp \frac{1}{3} \right) \left(\frac{59}{36} + \frac{1}{3} L_b + L_b^2 \right)\tag{3.32}$$

($L_b = \log(\mu_b^2/m_b^2)$ here and in the following two equations). We have determined the other entries by calculating two-loop matrix elements of the operators $Q_+, Q_-, Q_{3\dots 6}$ between

appropriate external states (see Figure 7), and find

$$\begin{aligned}
a_{33}^{(2)} &= 0, & a_{34}^{(2)} &= \frac{443}{54} - \frac{10}{9}L_b + \frac{10}{3}L_b^2, & a_{35}^{(2)} &= 0, \\
a_{36}^{(2)} &= -\frac{85}{108} + \frac{1}{9}L_b - \frac{1}{3}L_b^2; \\
a_{43}^{(2)} &= \frac{886}{243} - \frac{184}{81}L_b + \frac{40}{27}L_b^2, & a_{44}^{(2)} &= \frac{589}{162} - \frac{370}{81}L_b + \frac{37}{54}L_b^2, \\
a_{45}^{(2)} &= -\frac{85}{243} + \frac{4}{81}L_b - \frac{4}{27}L_b^2, & a_{46}^{(2)} &= -\frac{425}{648} + \frac{5}{54}L_b - \frac{5}{18}L_b^2; \\
a_{53}^{(2)} &= -\frac{452}{27} + \frac{80}{9}L_b, & a_{54}^{(2)} &= \frac{565}{27} + \frac{740}{9}L_b + \frac{100}{3}L_b^2, \\
a_{55}^{(2)} &= \frac{38}{27} - \frac{8}{9}L_b, & a_{56}^{(2)} &= -\frac{383}{54} - \frac{74}{9}L_b - \frac{10}{3}L_b^2; \\
a_{63}^{(2)} &= \frac{6874}{243} - \frac{88}{81}L_b + \frac{328}{27}L_b^2, & a_{64}^{(2)} &= -\frac{2651}{162} + \frac{5030}{81}L_b - \frac{220}{27}L_b^2, \\
a_{65}^{(2)} &= -\frac{826}{243} - \frac{128}{81}L_b - \frac{40}{27}L_b^2, & a_{66}^{(2)} &= -\frac{467}{162} - \frac{266}{27}L_b - \frac{23}{18}L_b^2.
\end{aligned} \tag{3.33}$$

For the dimension-eight operator we find the only non-vanishing contribution

$$\delta\tilde{r}_7^{(2)}(\mu_b) = -\frac{59}{54} - \frac{2}{9}L_b - \frac{2}{3}L_b^2 = \delta r_+^{(2)}(\mu_b). \tag{3.34}$$

3.4 Matching at the Charm-Quark Scale

At the scale $\mu_c = \mathcal{O}(m_c)$ the charm quark is removed from the theory as a dynamical degree of freedom, and the effective Lagrangian is now given by Equation (2.15). Requiring the equality of the Green's functions in both theories at the charm-quark scale leads to the matching condition

$$\sum_{i=+,-} \sum_{j=+,-,3}^6 C_i(\mu_c) C_j(\mu_c) \langle Q_i Q_j \rangle(\mu_c) + \tilde{C}_7(\mu_c) \tilde{Z}_{77} \langle \tilde{Q}_7 \rangle(\mu_c) = \frac{1}{32\pi^2} \tilde{C}_{S2}^{ct}(\mu_c) \tilde{Z}_{S2} \langle \tilde{Q}_{S2} \rangle(\mu_c), \tag{3.35}$$

which we use to determine the Wilson coefficient $\tilde{C}_{S2}^{ct}(\mu)$. To proceed, we parameterise the matrix elements in the following way:

$$\langle \tilde{Q}_7 \rangle = r_7 \langle \tilde{Q}_7 \rangle^{(0)}, \quad \langle \tilde{Q}_{S2} \rangle = r_{S2} \langle \tilde{Q}_{S2} \rangle^{(0)}, \quad \text{and} \quad \langle Q_i Q_j \rangle(\mu_c) = \frac{m_c^2(\mu_c)}{32\pi^2} r_{ij,S2} \langle \tilde{Q}_{S2} \rangle^{(0)}. \tag{3.36}$$

If we take into account the explicit factor of m_c^2/g^2 in the definition of \tilde{Q}_7 and expand the Wilson coefficient \tilde{C}_{S2}^{ct} as

$$\tilde{C}_{S2}^{ct}(\mu) = \frac{4\pi}{\alpha_s^{(3)}(\mu)} \tilde{C}_{S2}^{ct(0)}(\mu) + \tilde{C}_{S2}^{ct(1)}(\mu) + \frac{\alpha_s^{(3)}(\mu)}{4\pi} \tilde{C}_{S2}^{ct(2)}(\mu), \tag{3.37}$$

we find the following contributions to the matching:

$$\tilde{C}_{S_2}^{ct(0)}(\mu_c) = 2m_c^2(\mu_c)\tilde{C}_7^{(0)}(\mu_c), \quad (3.38)$$

$$\begin{aligned} \tilde{C}_{S_2}^{ct(1)}(\mu_c) &= 2m_c^2(\mu_c) \left[\tilde{C}_7^{(0)}(\mu_c) \left(r_7^{(1)} - r_{S_2}^{(1)} - \frac{2}{3} \log \frac{\mu_c^2}{m_c(\mu_c)^2} \right) + \tilde{C}_7^{(1)}(\mu_c) \right] \\ &\quad + m_c^2(\mu_c) C_i^{(0)}(\mu_c) C_j^{(0)}(\mu_c) r_{ij,S_2}^{(0)}, \end{aligned} \quad (3.39)$$

$$\begin{aligned} \tilde{C}_{S_2}^{ct(2)}(\mu_c) &= 2m_c^2(\mu_c) \left[\tilde{C}_7^{(0)}(\mu_c) \left(\delta\tilde{r}_7^{(2)}(\mu_c) + \frac{22}{9} - \frac{38}{3} \log \frac{\mu_c^2}{m_c(\mu_c)^2} \right) + \tilde{C}_7^{(2)}(\mu_c) \right] \\ &\quad + m_c^2(\mu_c) \left[C_i^{(0)}(\mu_c) C_j^{(0)}(\mu_c) (r_{ij,S_2}^{(1)} - r_{ij,S_2}^{(0)} r_{S_2}^{(1)}) \right. \\ &\quad \left. + C_i^{(0)}(\mu_c) C_j^{(1)}(\mu_c) r_{ij,S_2}^{(0)} + C_i^{(1)}(\mu_c) C_j^{(0)}(\mu_c) r_{ij,S_2}^{(0)} \right], \end{aligned} \quad (3.40)$$

where $\delta\tilde{r}_7^{(2)}(\mu_c)$ is given by Equation (3.34), but with μ_b and m_b replaced by μ_c and m_c , respectively. Notice the additional logarithms which we get by expressing $\alpha_s^{(f=4)}$ through $\alpha_s^{(f=3)}$. These terms, which are numerically tiny at NLO, have been neglected in Reference [7].

Furthermore, we expand the charm-quark mass defined at the scale μ_c , viz. $m_c(\mu_c)$, about $m_c(m_c)$ (see [13]):

$$x_c(\mu_c) = \kappa_c \left(1 + \frac{\alpha_s^{(4)}(\mu_c)}{4\pi} \xi_c^{(1)} + \left(\frac{\alpha_s^{(4)}(\mu_c)}{4\pi} \right)^2 \xi_c^{(2)} \right) x_c(m_c). \quad (3.41)$$

Here $\kappa_c = \eta_c^{24/25}$ with $\eta_c = \alpha_s^{(4)}(\mu_c)/\alpha_s^{(4)}(m_c)$ and

$$\begin{aligned} \xi_c^{(1)} &= \frac{15212}{1875} (1 - \eta_c^{-1}), \\ \xi_c^{(2)} &= \frac{966966391}{10546875} - \frac{231404944}{3515625} \eta_c^{-1} - \frac{272751559}{10546875} \eta_c^{-2} - \frac{128}{5} (1 - \eta_c^{-2}) \zeta_3. \end{aligned} \quad (3.42)$$

In order to evaluate the equations (3.38), we have to compute the finite parts of one- and two-loop Feynman diagrams of the type shown in Figure 8. In this way we find for $r_{\pm j,S_2}$ at one loop:

$$r_{\pm j,S_2}^{(0),T}(\mu_c) = \begin{pmatrix} 3 \log \left(\frac{\mu_c^2}{m_c^2} \right) - \frac{3}{2} & \frac{1}{2} - \log \left(\frac{\mu_c^2}{m_c^2} \right) \\ \frac{1}{2} - \log \left(\frac{\mu_c^2}{m_c^2} \right) & \log \left(\frac{\mu_c^2}{m_c^2} \right) - \frac{1}{2} \\ 0 & 0 \\ 0 & 0 \\ 96 \log \left(\frac{\mu_c^2}{m_c^2} \right) + 224 & -48 \log \left(\frac{\mu_c^2}{m_c^2} \right) - 112 \\ 8 \log \left(\frac{\mu_c^2}{m_c^2} \right) + \frac{56}{3} & 8 \log \left(\frac{\mu_c^2}{m_c^2} \right) + \frac{56}{3} \end{pmatrix} \quad (3.43)$$

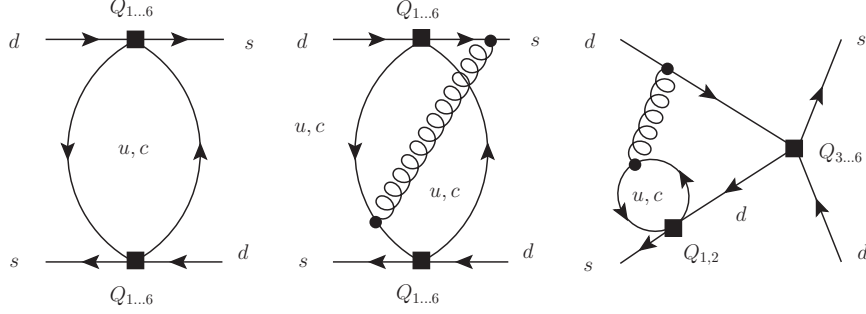


Figure 8: Sample one- and two-loop diagrams contributing to the matching at the charm-quark scale.

This result agrees with the one obtained in [7] after the appropriate basis transformation. A two-loop matching calculation yields

$$\begin{aligned}
& r_{\pm j, S_2}^{(1), T}(\mu_c) \\
&= \begin{pmatrix} 9 \log^2 \left(\frac{\mu_c^2}{m_c^2} \right) - 3 \log \left(\frac{\mu_c^2}{m_c^2} \right) - \zeta_2 + \frac{54926}{325} & -6 \log^2 \left(\frac{\mu_c^2}{m_c^2} \right) - 9 \log \left(\frac{\mu_c^2}{m_c^2} \right) + \frac{5}{3} \zeta_2 - \frac{89497}{1300} \\ -6 \log^2 \left(\frac{\mu_c^2}{m_c^2} \right) - 9 \log \left(\frac{\mu_c^2}{m_c^2} \right) + \frac{5}{3} \zeta_2 - \frac{89497}{1300} & 9 \log^2 \left(\frac{\mu_c^2}{m_c^2} \right) + 29 \log \left(\frac{\mu_c^2}{m_c^2} \right) + \frac{1}{3} \zeta_2 + \frac{11664}{325} \\ -4 \log^2 \left(\frac{\mu_c^2}{m_c^2} \right) + 28 \log \left(\frac{\mu_c^2}{m_c^2} \right) + \frac{23}{3} & -4 \log^2 \left(\frac{\mu_c^2}{m_c^2} \right) - 20 \log \left(\frac{\mu_c^2}{m_c^2} \right) - \frac{37}{3} \\ -\frac{37}{3} \log^2 \left(\frac{\mu_c^2}{m_c^2} \right) - \frac{59}{3} \log \left(\frac{\mu_c^2}{m_c^2} \right) - \frac{1531}{36} & \frac{11}{3} \log^2 \left(\frac{\mu_c^2}{m_c^2} \right) + \frac{85}{3} \log \left(\frac{\mu_c^2}{m_c^2} \right) + \frac{917}{36} \\ 344 \log^2 \left(\frac{\mu_c^2}{m_c^2} \right) + 920 \log \left(\frac{\mu_c^2}{m_c^2} \right) - \frac{64878}{65} & -376 \log^2 \left(\frac{\mu_c^2}{m_c^2} \right) - 1144 \log \left(\frac{\mu_c^2}{m_c^2} \right) - \frac{964226}{325} \\ -\frac{220}{3} \log^2 \left(\frac{\mu_c^2}{m_c^2} \right) - \frac{1636}{3} \log \left(\frac{\mu_c^2}{m_c^2} \right) - \frac{1015087}{195} & \frac{332}{3} \log^2 \left(\frac{\mu_c^2}{m_c^2} \right) + \frac{1412}{3} \log \left(\frac{\mu_c^2}{m_c^2} \right) + \frac{503161}{325} \end{pmatrix}. \tag{3.44}
\end{aligned}$$

This result is new and completes the matching onto the three-flavour theory. Now only a single operator contributes, and the renormalisation group evolution below the charm-quark scale is the same for the top-, the charm-, and the charm-top-quark contribution.

3.5 Renormalisation Group Equations below the Charm-Quark Threshold

The effective Hamiltonian valid below the charm-quark threshold contains only the single operator \tilde{Q}_{S_2} . The renormalisation group evolution is now the same for the three Wilson coefficients $\tilde{C}_{S_2}^j$, where $j = c, t, ct$, and is described by the evolution matrix corresponding to the anomalous dimension of \tilde{Q}_{S_2} :

$$\tilde{C}_{S_2}^j(\mu) = U(\mu, \mu_c) \tilde{C}_{S_2}^j(\mu_c). \tag{3.45}$$

By comparing (1.5) and (2.15), we see that we can express the coefficients η_{cc} , η_{tt} , η_{ct} as

$$\eta_{cc} = \frac{1}{m_c^2(m_c)} \tilde{C}_{S2}^{(c)}(\mu_c) [\alpha_s^{(3)}(\mu_c)]^{a_+} K_+^{-1}(\mu_c), \quad (3.46a)$$

$$\eta_{tt} = \frac{1}{M_W^2 S(x_t(m_t))} \tilde{C}_{S2}^{(t)}(\mu_c) [\alpha_s^{(3)}(\mu_c)]^{a_+} K_+^{-1}(\mu_c), \quad (3.46b)$$

$$\eta_{ct} = \frac{1}{2M_W^2 S(x_c(m_c), x_t(m_t))} \tilde{C}_{S2}^{(ct)}(\mu_c) [\alpha_s^{(3)}(\mu_c)]^{a_+} K_+^{-1}(\mu_c). \quad (3.46c)$$

The remaining μ -dependence present in (3.46), corresponding to the lower end of the evolution in Equation (3.45), is absorbed into $b(\mu)$, which equals

$$b(\mu) = [\alpha_s^{(3)}(\mu)]^{-a_+} K_+(\mu), \quad (3.47)$$

where

$$K_+(\mu) = \left(1 + J_+^{(1)} \frac{\alpha_s^{(3)}(\mu)}{4\pi} + J_+^{(2)} \left(\frac{\alpha_s^{(3)}(\mu)}{4\pi} \right)^2 \right), \quad (3.48)$$

and the exponent a_+ is the so-called *magic number* for the operator Q_+ (the magic numbers as well as the matrix J are defined for instance in [4]). This scale dependence is cancelled by the corresponding scale dependence of the hadronic matrix element.

3.6 Analytical Checks of our Calculation

Because the calculation of the NNLO contributions to η_{ct} is quite complex, we checked our results in several ways.

First of all the calculation of the $\mathcal{O}(100\,000)$ Feynman diagrams as well as the renormalisation, the computation of the anomalous dimensions and the matching, has been performed independently by the two of us, using a completely different setup of computer programs. On the one hand we use qgraf [26] for generating the diagrams; the evaluation of the integrals is then performed using the program packages q2e/exp/MATAD [27,28], where MATAD is written in FORM [29] and based on the Integration-By-Parts algorithm [30,31]. In addition, we have written our own FORM routine in order to evaluate two-loop diagrams with an arbitrary number of (possibly vanishing) masses, using the algorithm described in [14,32]. On the other hand, all calculations have been performed using an completely independent setup, based on Feynarts [33] and Mathematica.

As a check of our calculation, we verified that all anomalous dimensions, Wilson coefficients, and matrix elements are independent of the gauge-fixing parameter ξ . Because of the complexity of the analytical expressions, for the three-loop penguin insertions we kept only the first power in ξ for our check.

Another very useful check is the locality of the counterterms, which is an implication of renormalisability. In a mass independent renormalisation scheme this means that the

M_W	80.398(25) GeV	[2]	$\alpha_s(M_Z)$	0.1176(20)	[2]
$m_t(m_t)$	163.5(1.3) GeV	[34]	F_K	156.1(8) MeV	[35]
$m_b(m_b)$	4.163(16) GeV	[36]	G_F	$1.166\,37(1) \times 10^{-5} \text{GeV}^{-2}$	[2]
$m_c(m_c)$	1.286(13) GeV	[36]	λ	0.2255(7)	[35]
M_K	497.614(24) MeV	[2]	$ V_{cb} $	$4.12(11) \times 10^{-2}$	[2]
κ_ϵ	0.94(2)	[3]	M_{B_d}	5.2795(3) GeV	[2]
ΔM_K	5.292(9)/ns	[2]	M_{B_s}	5.3663(6) GeV	[2]
ΔM_d	0.507(5)/ps	[2]	ΔM_s	17.77(12)/ps	[2]
ξ_s	1.243(28)	[9]	η_{tt}	0.5765(65)	[8]
\hat{B}_K	0.725(26)	[9]	η_{cc}	1.43(23)	[7]
$\sin 2\beta$	0.671(23)	[2]			

Table 1: Input parameters used in our numerical analysis.

renormalisation factors Z depend on μ only through the coupling constants. We have checked this explicitly and found μ -independence of all our renormalisation constants.

We have also checked analytically that η_{ct} is independent of the matching scales μ_W , μ_b , and μ_c to the considered order of the strong coupling constant, by expanding the full solution of the renormalisation group equations about the respective matching scale.

As a cross-check, we confirm the NLO results of Herrlich and Nierste [7] for the first time.

4 Discussion and Numerics

In this section we present the numerical value of η_{ct} at NNLO and discuss the theoretical uncertainty, as well as the impact on ϵ_K . Our input parameters are collected in Table 1.

The theoretical uncertainty of η_{ct} is related to the truncation of the perturbation series. We estimate it by considering the remaining scale dependence, the different methods to evaluate the running strong coupling constant, and the size of the NNLO corrections. Varying μ_c from 1 to 2 GeV and μ_W from 40 to 200 GeV, we find the following numerical value at NNLO,

$$\eta_{ct} = 0.494 \pm 0.044_{\mu_c} \pm 0.013_{\mu_W} \pm 0.006_{\alpha_s} \pm 0.001_{m_c} \pm 0.0002_{m_t}, \quad (4.1)$$

where we also display the parametric uncertainties stemming from the experimental error on α_s , m_c , and m_t . The dependence on the scale μ_b is completely negligible.

The dependence on the electroweak matching scale μ_W is shown in Figure 9. We have plotted η_{ct} as a function of μ_W in the range from 40 GeV to 200 GeV, where we fixed the other scales as $\mu_b = 5$ GeV and $\mu_c = 1.5$ GeV, respectively. The relatively weak residual dependence on μ_W at NLO is slightly increased at NNLO. By contrast, the dependence on μ_b , which is shown in Figure 10, fixing $\mu_W = 80$ GeV and $\mu_c = 1.5$ GeV, is completely

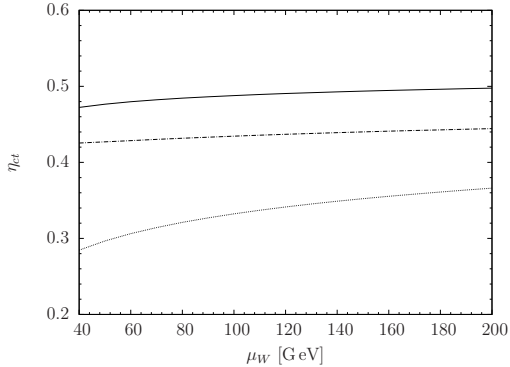


Figure 9: η_{ct} as a function of μ_W at LO (dotted line), NLO (dashed-dotted line), and NNLO QCD (solid line).

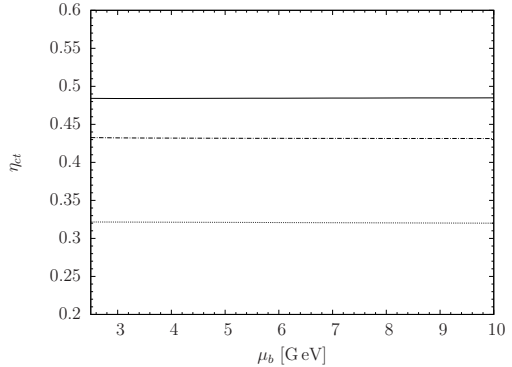


Figure 10: η_{ct} as a function of μ_b at LO (dotted line), NLO (dashed-dotted line), and NNLO QCD (solid line).

negligible. The dependence on the scale μ_c is shown in Figure 11, where we vary μ_c in the range from 1 to 2 GeV, fixing $\mu_W = 80$ GeV and $\mu_b = 5$ GeV. In addition, we have plotted η_{ct} corresponding to three different possibilities of calculating $\alpha_s(\mu_c)$ from the experimental input value of $\alpha_s(M_Z)$: One method (1) is to solve the renormalisation group equation for α_s numerically. Furthermore, it is possible to compute α_s by first determining the scale parameter Λ_{QCD} . This can be achieved by using the explicit solution for Λ_{QCD} without expansion in α_s (method 2) or by iteratively solving this equation for Λ_{QCD} and from this value determining α_s (method 3). The dashed, dotted, and dashed-dotted lines in Figure 11, each of them representing the NLO result for η_{ct} , correspond to these three possibilities of determining α_s , respectively. We used the mathematica package RunDec [37] for the numerical evaluation. Note that the difference between these three methods vanishes almost entirely at NNLO. On the other hand, at NLO the effect is sizeable and thus contributes to the theoretical uncertainty. Varying μ_c and μ_W in the same range as above, we find at NLO

$$\eta_{ct}^{\text{NLO}} = 0.455 \pm 0.068_{\mu_c} \pm 0.009_{\mu_W} \pm 0.0004_{\alpha_s} \pm 0.002_{m_c} \pm 0.0003_{m_t}, \quad (4.2)$$

where the error indicated by the subscript “ μ_c ” includes the effect of the three ways of determining α_s . For the variation of the scale μ_W we have used only method 1 for evaluating α_s in order to avoid double-counting of the related uncertainty⁵.

Again we have included the parametric uncertainties related to α_s , m_c , and m_t .

The authors of Reference [7] have varied μ_c in the smaller range from 1.1 to 1.6 GeV, using a procedure equivalent to method 3 above for determining α_s . By looking at the explicit values of η_{ct} in Figure 11 we see that the two error bands at NLO and NNLO, resulting from this smaller range of μ_c , have almost no overlap. Now, with the NNLO results at hand, we see that our range for μ_c leads to a better estimate of the theoretical uncertainty.

⁵Otherwise the error would amount to $\pm 0.018_{\mu_W}$.

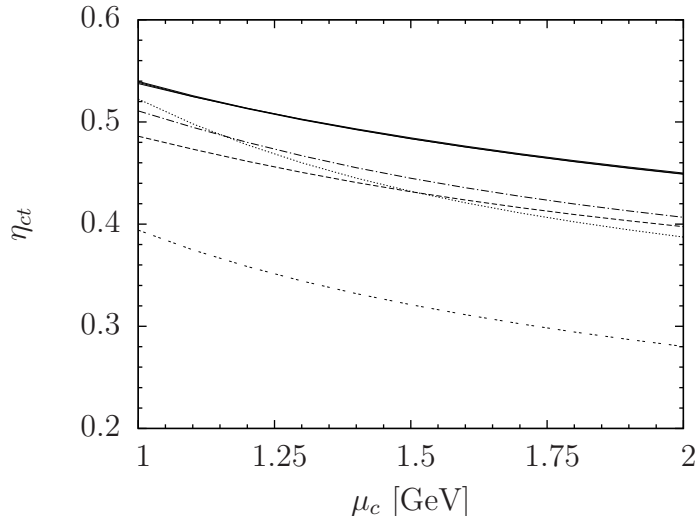


Figure 11: η_{ct} as a function of μ_c . The LO result is represented by the double-dotted line. The dashed, dotted, and dashed-dotted lines correspond to the NLO value of η_{ct} , with α_s evaluated by method 1, 2, and 3, explained in the text. The solid lines show the corresponding NNLO results; the ambiguity is almost cancelled.

Looking at Figure 11, it is striking that the scale dependence of the NLO result is barely reduced at NNLO. In order to understand this behaviour, let us look at the remaining μ_c dependence, which is the most pronounced, in more detail. It originates from terms proportional to higher powers of α_s times logarithms of the renormalisation scale that are contained in the explicit solutions of the renormalisation group equations. These terms are only partially cancelled due to our truncating the perturbative expansion of the matrix elements at the charm-quark scale.

We have separated the contributions to η_{ct} of the different Wilson coefficients multiplying the matrix elements at the charm-quark scale (cf. Equation (3.38)). To this end we have chosen the operator basis as in Reference [7], where we use the diagonal operator basis only in one dimension-six subspace, and Q_1, \dots, Q_6 in the other. It turns out that only one contribution, proportional to the combination C_-C_2 , shows a strong scale dependence. Although the size of the individual contributions certainly depends on the chosen renormalisation scheme, the general pattern is independent of this convention. It is related to the vanishing of the entry in the LO anomalous dimension tensor corresponding to the two operators Q_- and Q_2 . This incidence leads to a behaviour of the scale dependence for this single combination which would be expected from a NLO calculation, and dominates the scale dependence of the NNLO result.

Finally we remark that the absolute value of the NNLO correction is of the same order of magnitude as the range of η_{ct} at NNLO in the interval $\mu_c = 1 \dots 2$ GeV, so that using the size of the NNLO corrections as an estimate of the theoretical uncertainty yields approximately the same error as using the scale variation in the quoted interval.

As a summary of the discussion above, we give the following final estimate for the

charm-top-quark contribution to ϵ_K at NNLO:

$$\eta_{ct} = 0.494 \pm 0.046. \quad (4.3)$$

(For comparison, an error estimate using a range for μ_c as in Reference [7] would yield $\eta_{ct} = 0.500 \pm 0.025$.) The parametric uncertainty is essentially negligible with respect to the theoretical uncertainty. Compared to our NLO value,

$$\eta_{ct}^{\text{NLO}} = 0.455 \pm 0.069, \quad (4.4)$$

this corresponds to a positive shift of approximately 7%:

Before we conclude this section, we study the impact of our calculation on the prediction of $|\epsilon_K|$. To this end we use the following formula⁶ [38, 39]:

$$|\epsilon_K| = \kappa_\epsilon C_\epsilon \hat{B}_K |V_{cb}|^2 \lambda^2 \bar{\eta} (|V_{cb}|^2 (1 - \bar{\rho}) \eta_{tt} S(x_t) + \eta_{ct} S(x_c, x_t) - \eta_{cc} S(x_c)), \quad (4.5)$$

where

$$C_\epsilon = \frac{G_F^2 F_K^2 M_{K^0} M_W^2}{6\sqrt{2}\pi^2 \Delta M_K}. \quad (4.6)$$

We write $\bar{\eta} = R_t \sin \beta$ and $1 - \bar{\rho} = R_t \cos \beta$, where R_t is given by

$$R_t \approx \frac{\xi_s}{\lambda} \sqrt{\frac{M_{B_s}}{M_{B_d}}} \sqrt{\frac{\Delta M_d}{\Delta M_s}} \quad (4.7)$$

and $\xi_s = (F_{B_s} \sqrt{\hat{B}_s}) / (F_{B_d} \sqrt{\hat{B}_d})$ is a ratio of B meson decay constants and bag factors that can be computed on the lattice with high precision [9]. Using the numerical values given in Table 1, we obtain

$$|\epsilon_K| = (1.99 \pm 0.04_{\eta_{cc}} \pm 0.02_{\eta_{tt}} \pm 0.08_{\eta_{ct}} \pm 0.11_{\text{LD}} \pm 0.20_{\text{parametric}}) \times 10^{-3}. \quad (4.8)$$

The first three errors correspond to η_{cc} , η_{tt} , η_{ct} , respectively. The error indicated by LD originates from the long-distance contribution, namely ξ_s , \hat{B}_K , and κ_ϵ , which account for 41%, 37%, and 22% of the long-distance error, respectively. The main share of the parametric error stems from $|V_{cb}|$ (54%) and $\sin(2\beta)$ (21%), while all other contributions are well below 10%. All errors have been added in quadrature.

Compared to the prediction using the NLO value η_{ct}^{NLO} ,

$$|\epsilon_K^{\text{NLO}}| = (1.92 \pm 0.04_{\eta_{cc}} \pm 0.02_{\eta_{tt}} \pm 0.11_{\eta_{ct}} \pm 0.11_{\text{LD}} \pm 0.20_{\text{parametric}}) \times 10^{-3}, \quad (4.9)$$

this corresponds to a shift by 3.3%.

⁶A term proportional to $\text{Re}\lambda_t/\text{Re}\lambda_c = \mathcal{O}(\lambda^4)$ has been neglected in Equation (4.5) (see Reference [38]).

5 Conclusion

We have performed a complete NNLO QCD analysis of the charm-top-quark contribution η_{ct} to the $|\Delta S| = 2$ effective Hamiltonian $\mathcal{H}_{f=3}^{|\Delta S|=2}$. We confirm the analytical results for η_{ct} obtained at NLO in Reference [7] for the first time.

Some of our results are useful beyond η_{ct} . The anomalous dimension of the operator \tilde{Q}_{S2} can be employed to compute the large NNLO logarithms of $B^0 - \bar{B}^0$ mixing and comprise part of a NNLO calculation of η_{tt} . The NNLO matching corrections at the bottom-quark threshold have further applications in Kaon physics.

Our numerical results for η_{ct} can be summarised by a 7% positive shift in the NNLO prediction with respect to the NLO value, leading to $\eta_{ct} = 0.494 \pm 0.046$. This corresponds to an enhancement of ϵ_K by roughly 3.3%, yielding $|\epsilon_K| = (1.99 \pm 0.25) \times 10^{-3}$. With our calculation we solidified the theory prediction of ϵ_K , strengthening its role as an important constraint for models of new physics.

Acknowledgements

JB would like to thank Ulrich Nierste for suggesting the topic, Matthias Steinhauser for providing us with an updated version of MATAD, and Emmanuel Stamou for his help in improving our FORM routines. We also thank Ulrich Nierste for constant encouragement and discussions, and Andrzej Buras, Ulrich Nierste, Guido Bell and Emmanuel Stamou for their careful reading of the manuscript.

This research was supported by the DFG cluster of excellence “Origin and Structure of the Universe”. The work of JB was supported by the EU Marie-Curie grant MIRC-CT-2005-029152, BMBF grant 05 HT6VKB, and by the DFG-funded “Graduiertenkolleg Hochenergiephysik und Teilchenastrophysik” at the University of Karlsruhe. MG thanks the Galileo Galilei Institute for Theoretical Physics for the hospitality and the INFN for partial support during the completion of this work.

A Change of the Operator Basis

In this appendix we examine how the Wilson coefficients and the anomalous dimensions transform under a change of the operator basis. This is important for two reasons: In order to find a compact form for the renormalisation group equations for double operator insertions, we have seen it to be useful to work in a diagonal operator basis in the subspace of current-current operators. However, the calculation of the dimension-six anomalous dimensions and Wilson coefficients has been performed in the literature in the basis given in [4, 12]. Moreover, we had to transform our results in order to compare them with results that are available in the literature and have been calculated using yet another operator basis [7].

As is well known, a general change of the operator basis consists of a linear transformation and a corresponding change of the renormalisation scheme [4]. Therefore, let us

first as a preparation derive the transformation properties of the anomalous dimensions for an arbitrary change of the renormalisation scheme. This generalises the already known results. Suppose we perform the following change of scheme for the Wilson coefficients

$$C_i \rightarrow C'_i = C_j \rho_{ji}^{-1}, \quad (\text{A.1})$$

$$\tilde{C}_k \rightarrow \tilde{C}'_k = \tilde{C}_j \tilde{\rho}_{jk}^{-1} - C_l C_m \hat{\rho}_{lm,k}. \quad (\text{A.2})$$

As before, we have denoted Wilson coefficients belonging to dimension-eight operators with a tilde and those belonging to dimension-six operators without superscript. Furthermore, we introduced the parameters ρ , $\tilde{\rho}$ and $\hat{\rho}$, which parameterise the finite transformations:

$$\rho_{ij} = \delta_{ij} - \frac{\alpha_s}{4\pi} \rho_{ij}^{(1)} - \left(\frac{\alpha_s}{4\pi}\right)^2 \left(\rho_{ij}^{(2)} - \rho_{ik}^{(1)} \rho_{kj}^{(1)}\right) + \mathcal{O}(\alpha_s^3), \quad (\text{A.3})$$

$$\tilde{\rho}_{ij} = \delta_{ij} - \frac{\alpha_s}{4\pi} \tilde{\rho}_{ij}^{(1)} - \left(\frac{\alpha_s}{4\pi}\right)^2 \left(\tilde{\rho}_{ij}^{(2)} - \tilde{\rho}_{ik}^{(1)} \tilde{\rho}_{kj}^{(1)}\right) + \mathcal{O}(\alpha_s^3), \quad (\text{A.4})$$

$$\hat{\rho}_{lm,k} = \frac{\alpha_s}{4\pi} \hat{\rho}_{lm,k}^{(1)} + \left(\frac{\alpha_s}{4\pi}\right)^2 \hat{\rho}_{lm,k}^{(2)} + \mathcal{O}(\alpha_s^3). \quad (\text{A.5})$$

Then, in order for the effective Hamiltonian of the form

$$H_{\text{eff}} = C_i Z_{ij} Q_j + (\tilde{C}_i \tilde{Z}_{ik} + C_i C_j \hat{Z}_{ij,k}) \tilde{Q}_k \quad (\text{A.6})$$

to stay invariant, the renormalisation constants must transform as

$$Z_{ij} \rightarrow Z'_{ij} = \rho_{ik} Z_{kj}, \quad (\text{A.7})$$

$$\tilde{Z}_{ij} \rightarrow \tilde{Z}'_{ij} = \tilde{\rho}_{ik} \tilde{Z}_{kj}, \quad (\text{A.8})$$

$$\hat{Z}_{ij,k} \rightarrow \hat{Z}'_{ij,k} = \rho_{il} \rho_{jm} \hat{Z}_{lm,k} + \rho_{il} \rho_{jm} \hat{\rho}_{lm,p} \tilde{\rho}_{pq} \tilde{Z}_{qk}. \quad (\text{A.9})$$

The transformation of the anomalous dimensions can now be obtained by inserting the transformed renormalisation constants into the defining equation for the anomalous dimension matrix (3.5), and the anomalous dimension tensor (3.7), respectively. In this way we obtain the well-known results for the case of single insertions [4, 40, 41]:

$$\gamma'^{(0)} = \gamma^{(0)}, \quad (\text{A.10})$$

$$\gamma'^{(1)} = \gamma^{(1)} - [\rho^{(1)}, \gamma^{(0)}] - 2\beta_0 \rho^{(1)}, \quad (\text{A.11})$$

$$\begin{aligned} \gamma'^{(2)} = & \gamma^{(2)} - [\rho^{(2)}, \gamma^{(0)}] - [\rho^{(1)}, \gamma^{(1)}] + \rho^{(1)} [\rho^{(1)}, \gamma^{(0)}] \\ & - 4\beta_0 \rho^{(2)} - 2\beta_1 \rho^{(1)} + 2\beta_0 \rho^{(1)} \rho^{(1)}. \end{aligned} \quad (\text{A.12})$$

The general transformation law for the anomalous dimension tensor for double insertion reads:⁷

$$\hat{\gamma}'_{ij,k}{}^{(0)} = \gamma_{ij,k}^{(0)}, \quad (\text{A.13})$$

$$\begin{aligned} \hat{\gamma}'_{ij,k}{}^{(1)} = & \gamma_{ij,k}^{(1)} + \hat{\rho}_{ij,l}^{(1)} \tilde{\gamma}_{lk}^{(0)} + 2\hat{\rho}_{ij,k}^{(1)} \beta_0 + \hat{\gamma}_{ij,l}^{(0)} \tilde{\rho}_{lk}^{(1)} \\ & - \left\{ \gamma_{il}^{(0)} \delta_{jm} + \delta_{il} \gamma_{jm}^{(0)} \right\} \hat{\rho}_{lm,k}^{(1)} - \left\{ \rho_{il}^{(1)} \delta_{jm} + \delta_{il} \rho_{jm}^{(1)} \right\} \hat{\gamma}_{lm,k}^{(0)}. \end{aligned} \quad (\text{A.14})$$

⁷Note that additional finite contributions arise if we include the factor of m_c^2/g^2 in the definition of the dimension-eight operators.

Let us now examine how the anomalous dimensions and the Wilson coefficients change under a basis transformation. In four space-time dimensions, a change of n dimension-six operators Q and m dimension-eight operators \tilde{Q} is simply given by a linear transformation

$$Q_i \rightarrow Q'_i = R_{ij}Q_j, \quad \tilde{Q}_i \rightarrow \tilde{Q}'_i = \tilde{R}_{ij}\tilde{Q}_j, \quad (\text{A.15})$$

described by matrices $R \in \text{GL}(n)$, $\tilde{R} \in \text{GL}(m)$. Under this transformation the renormalisation constants change according to

$$Z'_{ij} = R_{ik}Z_{kl}R_{lj}^{-1}, \quad \tilde{Z}'_{ij} = \tilde{R}_{ik}\tilde{Z}_{kl}\tilde{R}_{lj}^{-1}, \quad \hat{Z}'_{kn,l} = R_{kk'}R_{nn'}\hat{Z}_{k'n',l'}\tilde{R}_{l'l}^{-1}. \quad (\text{A.16})$$

In general, the situation is more complicated because of the presence of evanescent operators. As explained in detail in Reference [4], a change of the operator basis consists of a linear transformation and a finite renormalisation; the latter is needed in order to restore the standard $\overline{\text{MS}}$ definition of the renormalisation constants.

We can write a general transformation among all dimension-six operators as

$$\begin{pmatrix} Q' \\ E' \end{pmatrix} = \begin{pmatrix} R & 0 \\ 0 & M \end{pmatrix} \begin{pmatrix} 1 & 0 \\ \epsilon U + \epsilon^2 V & 1 \end{pmatrix} \begin{pmatrix} 1 & W \\ 0 & 1 \end{pmatrix} \begin{pmatrix} Q \\ E \end{pmatrix}, \quad (\text{A.17})$$

where the matrices R and M parameterise a linear transformation among the physical and evanescent operators Q and E , respectively, W parameterises the addition of multiples of evanescent operators to the physical operators, and U and V parameterise the addition of multiples of ϵ and ϵ^2 times physical operators to the evanescent operators, respectively. We apply a transformation of the same form to the dimension-eight operators, where we denote the corresponding matrices by a tilde, as before. The finite renormalisation constants can now be determined by requiring that an effective amplitude of the form $C_i Z_{ij} \langle Q_j \rangle + (\tilde{C}_l \tilde{Z}_{lk} + C_i C_j \tilde{Z}_{ij,k}) \langle \tilde{Q}_k \rangle$ be invariant under the basis transformation and be renormalised according to the $\overline{\text{MS}}$ prescription.

Let us start with the anomalous dimension matrices for the mixing of dimension-six into dimension-six operators. The finite renormalisation induced by the change (A.17) is given by [4, 13]

$$\begin{aligned} Z'_{QQ}{}^{(1,0)} &= R \left[W Z_{EQ}{}^{(1,0)} - \left(Z_{QE}{}^{(1,1)} + W Z_{EE}{}^{(1,1)} - \frac{1}{2} \gamma^{(0)} W \right) U \right] R^{-1}, \\ Z'_{QQ}{}^{(2,0)} &= -R \left(Z_{QE}{}^{(2,1)} U + Z_{QE}{}^{(2,2)} V - \frac{1}{2} Z_{QE}{}^{(1,1)} V \gamma^{(0)} \right) R^{-1}, \end{aligned} \quad (\text{A.18})$$

where

$$Z_{QE}{}^{(2,2)} = \frac{1}{2} \left(Z_{QE}{}^{(1,1)} Z_{EE}{}^{(1,1)} + \frac{1}{2} \gamma^{(0)} Z_{QE}{}^{(1,1)} - \beta_0 Z_{QE}{}^{(1,1)} \right). \quad (\text{A.19})$$

We have set W to zero in the second line of Equation (A.18) as these terms are not needed in our work. We now find the transformation law for the anomalous dimension matrices

in a straightforward manner using Equations (A.10) to (A.12):

$$\begin{aligned}
\gamma'^{(0)} &= R\gamma^{(0)}R^{-1}, \\
\gamma'^{(1)} &= R\gamma^{(1)}R^{-1} - \left[Z'_{QQ}{}^{(1,0)}, \gamma'^{(0)} \right] - 2\beta_0 Z'_{QQ}{}^{(1,0)}, \\
\gamma'^{(2)} &= R\gamma^{(2)}R^{-1} - \left[Z'_{QQ}{}^{(2,0)}, \gamma'^{(0)} \right] - \left[Z'_{QQ}{}^{(1,0)}, \gamma'^{(1)} \right] + \left[Z'_{QQ}{}^{(1,0)}, \gamma'^{(0)} \right] Z'_{QQ}{}^{(1,0)} \\
&\quad - 4\beta_0 Z'_{QQ}{}^{(2,0)} - 2\beta_1 Z'_{QQ}{}^{(1,0)} + 2\beta_0 \left(Z'_{QQ}{}^{(1,0)} \right)^2.
\end{aligned} \tag{A.20}$$

The Wilson coefficients change according to

$$C'(\mu) = \left[1 + \frac{\alpha_s(\mu)}{4\pi} Z'_{QQ}{}^{(1,0)} + \left(\frac{\alpha_s(\mu)}{4\pi} \right)^2 Z'_{QQ}{}^{(2,0)} \right]^T (R^{-1})^T C(\mu). \tag{A.21}$$

Clearly, the transformation law of the anomalous dimension matrix describing the mixing among the dimension-eight operators themselves is given by a formula completely analogous to (A.20). In order to find the transformation law of the anomalous dimension tensor, describing the mixing of dimension-six into dimension-eight operators, and of the dimension-eight Wilson coefficients, we apply the same method as above. In addition to the finite renormalisation constants (A.18), we now get extra finite contributions to \hat{Z} :

$$\begin{aligned}
\hat{Z}'_{ij,k}{}^{(1,0)} &= R_{im}R_{jn} \left(\hat{Z}_{mn,l}{}^{(1,1)} \tilde{W}_{l'p} \tilde{U}_{l'p} - \hat{Z}_{mn,l}{}^{(1,1)} \tilde{U}_{lp} + W_{ml} \hat{Z}_{ln,p}{}^{(1,0)} + W_{nl} \hat{Z}_{ml,p}{}^{(1,0)} \right. \\
&\quad \left. - W_{il} \hat{Z}_{ln,m}{}^{(1,1)} \tilde{U}_{mp} - W_{nl} \hat{Z}_{il,m}{}^{(1,1)} \tilde{U}_{mp} \right) \tilde{R}_{pk}^{-1}.
\end{aligned} \tag{A.22}$$

Here the indices i, j , and k correspond to physical operators only. These expressions have never been given explicitly in the literature before. The anomalous dimension tensor then transforms according to

$$\gamma'_{ij,k}{}^{(0)} = R_{im}R_{jn} \gamma_{mn,l}{}^{(0)} \tilde{R}_{lk}^{-1}, \tag{A.23}$$

$$\begin{aligned}
\gamma'_{ij,k}{}^{(1)} &= R_{im}R_{jn} \gamma_{mn,l}{}^{(1)} \tilde{R}_{lk}^{-1} + \hat{Z}'_{ij,l}{}^{(1,0)} \tilde{\gamma}'_{lk}{}^{(0)} + 2\hat{Z}'_{ij,k}{}^{(1,0)} \beta_0 + \hat{\gamma}'_{ij,l}{}^{(0)} \tilde{Z}'_{lk}{}^{(1,0)} \\
&\quad - \left\{ \gamma'_{il}{}^{(0)} \delta_{jm} + \delta_{il} \gamma'_{jm}{}^{(0)} \right\} \hat{Z}'_{lm,k}{}^{(1,0)} - \left\{ Z'_{il}{}^{(1,0)} \delta_{jm} + \delta_{il} Z'_{jm}{}^{(1,0)} \right\} \hat{\gamma}'_{lm,k}{}^{(0)},
\end{aligned} \tag{A.24}$$

as can be derived easily from Equations (A.13) and (A.14). A special case of these formulas has been derived in Reference [15]. Using the definition (A.2), we see that the dimension-eight Wilson coefficients transform as

$$\begin{aligned}
\tilde{C}'_k(\mu) &= \tilde{C}_i(\mu) \tilde{R}_{ij}^{-1} \left[\delta_{jk} + \frac{\alpha_s(\mu)}{4\pi} \tilde{Z}'_{jk}{}^{(1,0)} \right] \\
&\quad - C_i(\mu) R_{im}^{-1} C_j(\mu) R_{jn}^{-1} \left[\frac{\alpha_s(\mu)}{4\pi} \hat{Z}'_{mn,k}{}^{(1,0)} \right].
\end{aligned} \tag{A.25}$$

Transformation to the Traditional Operator Basis

The calculation of the NLO QCD corrections to η_{ct} in [7] has been performed in a different basis for the physical operators than the one chosen by us. It is given by

$$\begin{aligned}
Q_1'^{qq'} &= (\bar{s}_L^\alpha \gamma_\mu q_L^\alpha) \otimes (\bar{q}'_L^\beta \gamma^\mu d_L^\beta), \\
Q_2'^{qq'} &= (\bar{s}_L^\alpha \gamma_\mu q_L^\beta) \otimes (\bar{q}'_L^\beta \gamma^\mu d_L^\alpha), \\
Q_3' &= (\bar{s}_L^\alpha \gamma_\mu d_L^\alpha) \otimes \sum_q (\bar{q}'_L^\beta \gamma^\mu q_L^\beta), \\
Q_4' &= (\bar{s}_L^\alpha \gamma_\mu d_L^\beta) \otimes \sum_q (\bar{q}'_L^\beta \gamma^\mu q_L^\alpha), \\
Q_5' &= (\bar{s}_L^\alpha \gamma_\mu d_L^\alpha) \otimes \sum_q (\bar{q}'_R^\beta \gamma^\mu q_R^\beta), \\
Q_6' &= (\bar{s}_L^\alpha \gamma_\mu d_L^\beta) \otimes \sum_q (\bar{q}'_R^\beta \gamma^\mu q_R^\alpha).
\end{aligned} \tag{A.26}$$

Note that we have expressed the operators in terms of left- and right-handed fermion fields, in contrast to the definition used in [7]. The evanescent operators chosen in [7] are equivalent to the following set of operators:

$$\begin{aligned}
E_1'^{qq'(1)} &= (\bar{s}_L^\alpha \gamma_{\mu_1 \mu_2 \mu_3} q_L^\alpha) \otimes (\bar{q}'_L^\beta \gamma^{\mu_1 \mu_2 \mu_3} d_L^\beta) - (16 - 4\epsilon) Q_1'^{qq'}, \\
E_2'^{qq'(1)} &= (\bar{s}_L^\alpha \gamma_{\mu_1 \mu_2 \mu_3} q_L^\beta) \otimes (\bar{q}'_L^\beta \gamma^{\mu_1 \mu_2 \mu_3} d_L^\alpha) - (16 - 4\epsilon) Q_2'^{qq'}, \\
E_3'^{(1)} &= (\bar{s}_L^\alpha \gamma_{\mu_1 \mu_2 \mu_3} d_L^\alpha) \otimes \sum_q (\bar{q}'_L^\beta \gamma^{\mu_1 \mu_2 \mu_3} q_L^\beta) - (16 - 4\epsilon) Q_3', \\
E_4'^{(1)} &= (\bar{s}_L^\alpha \gamma_{\mu_1 \mu_2 \mu_3} d_L^\beta) \otimes \sum_q (\bar{q}'_L^\beta \gamma^{\mu_1 \mu_2 \mu_3} q_L^\alpha) - (16 - 4\epsilon) Q_4', \\
E_5'^{(1)} &= (\bar{s}_L^\alpha \gamma_{\mu_1 \mu_2 \mu_3} d_L^\alpha) \otimes \sum_q (\bar{q}'_R^\beta \gamma^{\mu_1 \mu_2 \mu_3} q_R^\beta) - (4 + 4\epsilon) Q_5', \\
E_6'^{(1)} &= (\bar{s}_L^\alpha \gamma_{\mu_1 \mu_2 \mu_3} d_L^\beta) \otimes \sum_q (\bar{q}'_R^\beta \gamma^{\mu_1 \mu_2 \mu_3} q_R^\alpha) - (4 + 4\epsilon) Q_6'.
\end{aligned} \tag{A.27}$$

It turns out that in order to transform from our operator basis to the traditional one the following four evanescent operators must be introduced at the one-loop level in addition to the evanescent operators given in Equation (2.10) (see Reference [4]):

$$\begin{aligned}
E_5^{(1)} &= (\bar{s}_L \gamma_\mu d_L) \otimes \sum_q (\bar{q} \gamma^\mu \gamma_5 q) - \frac{5}{3} Q_3 + \frac{1}{6} Q_5, \\
E_6^{(1)} &= (\bar{s}_L \gamma_\mu T^a d_L) \otimes \sum_q (\bar{q} \gamma^\mu \gamma_5 T^a q) - \frac{5}{3} Q_4 + \frac{1}{6} Q_6, \\
E_7^{(1)} &= (\bar{s}_L \gamma_{\mu_1 \mu_2 \mu_3} d_L) \otimes \sum_q (\bar{q} \gamma^{\mu_1 \mu_2 \mu_3} \gamma_5 q) - \frac{32}{3} Q_3 + \frac{5}{3} Q_5, \\
E_8^{(1)} &= (\bar{s}_L \gamma_{\mu_1 \mu_2 \mu_3} T^a d_L) \otimes \sum_q (\bar{q} \gamma^{\mu_1 \mu_2 \mu_3} \gamma_5 T^a q) - \frac{32}{3} Q_4 + \frac{5}{3} Q_6,
\end{aligned} \tag{A.28}$$

The transformation matrices R , M , W , and U representing the basis transformation according to Equation (A.17), as well as the finite renormalisation induced by this transformation, can be found in [4]. The parts of the transformation matrices relevant to us are

given by⁸

$$R = \begin{pmatrix} 2 & \frac{1}{3} & 0 & 0 & 0 & 0 \\ 0 & 1 & 0 & 0 & 0 & 0 \\ 0 & 0 & -\frac{1}{3} & 0 & \frac{1}{12} & 0 \\ 0 & 0 & -\frac{1}{9} & -\frac{2}{3} & \frac{1}{36} & \frac{1}{6} \\ 0 & 0 & \frac{4}{9} & 0 & -\frac{1}{12} & 0 \\ 0 & 0 & \frac{4}{9} & \frac{8}{3} & -\frac{1}{36} & -\frac{1}{6} \end{pmatrix}, \quad M = \begin{pmatrix} 2 & \frac{1}{3} & 0 & 0 & 0 & 0 & 0 & 0 \\ 0 & 1 & 0 & 0 & 0 & 0 & 0 & 0 \\ 0 & 0 & 0 & 0 & 8 & 0 & -\frac{1}{2} & 0 \\ 0 & 0 & 0 & 0 & \frac{8}{3} & 16 & -\frac{1}{6} & -1 \\ 0 & 0 & 0 & 0 & -2 & 0 & \frac{1}{2} & 0 \\ 0 & 0 & 0 & 0 & -\frac{2}{3} & -4 & \frac{1}{6} & 1 \end{pmatrix}, \quad (\text{A.29})$$

$$W = \begin{pmatrix} 0 & 0 & 0 & 0 & 0 & 0 & 0 & 0 \\ 0 & 0 & 0 & 0 & 0 & 0 & 0 & 0 \\ 0 & 0 & 0 & 0 & 0 & 0 & 0 & 0 \\ 0 & 0 & 0 & 0 & 0 & 0 & 0 & 0 \\ 0 & 0 & 0 & 0 & -6 & 0 & 0 & 0 \\ 0 & 0 & 0 & 0 & 0 & -6 & 0 & 0 \end{pmatrix}, \quad U = \begin{pmatrix} 0 & 0 & 0 & 0 & 0 & 0 \\ 0 & 0 & 0 & 0 & 0 & 0 \\ 0 & 0 & -112 & 0 & 16 & 0 \\ 0 & 0 & 0 & -112 & 0 & 16 \\ 0 & 0 & -\frac{10}{9} & 0 & \frac{1}{9} & 0 \\ 0 & 0 & 0 & -\frac{10}{9} & 0 & \frac{1}{9} \\ 0 & 0 & -\frac{136}{9} & 0 & \frac{10}{9} & 0 \\ 0 & 0 & 0 & -\frac{136}{9} & 0 & \frac{10}{9} \end{pmatrix}, \quad (\text{A.30})$$

whereas the matrix V vanishes. They correspond to the bases

$$Q' = (Q_1^{qq'}, Q_2^{qq'}, Q_3', \dots, Q_6'), \quad E' = (E_1'^{qq'(1)}, E_2'^{qq'(1)}, E_3'^{(1)}, \dots, E_6'^{(1)}), \quad (\text{A.31})$$

and

$$Q = (Q_1^{qq'}, Q_2^{qq'}, Q_3, \dots, Q_6), \quad E = (E_1^{qq'(1)}, E_2^{qq'(1)}, E_3^{(1)}, \dots, E_8^{(1)}) \quad (\text{A.32})$$

in the notation of (A.17). The one-loop contribution to the finite renormalisation in the dimension-six sector is given by

$$\hat{Z}'_{QQ}{}^{(1,0)} = \begin{pmatrix} 0 & 0 & 0 & 0 & 0 & 0 \\ 0 & 0 & 0 & 0 & 0 & 0 \\ 0 & 0 & \frac{178}{27} & -\frac{34}{9} & -\frac{164}{27} & \frac{20}{9} \\ 0 & 0 & 1 - \frac{f}{9} & \frac{f}{3} - \frac{25}{3} & -\frac{f}{9} - 2 & \frac{f}{3} + 6 \\ 0 & 0 & -\frac{160}{27} & \frac{16}{9} & \frac{146}{27} & -\frac{2}{9} \\ 0 & 0 & \frac{f}{9} - 2 & 6 - \frac{f}{3} & \frac{f}{9} + 3 & -\frac{f}{3} - \frac{11}{3} \end{pmatrix}. \quad (\text{A.33})$$

The finite renormalisation relevant for the mixing of dimension-six into dimension-eight operators has never been calculated before. We find

$$\hat{Z}'_{QQ, \hat{Q}_7}{}^{(1,0), T} = \begin{pmatrix} 0 & 0 & -20 & -\frac{20}{3} & 20 & \frac{20}{3} \\ 0 & 0 & -\frac{20}{3} & -\frac{20}{3} & \frac{20}{3} & \frac{20}{3} \end{pmatrix}. \quad (\text{A.34})$$

⁸An additional rotation must be performed in order to change to the ‘‘diagonal’’ operator basis. This does not affect the finite renormalisation.

Transformation to the Diagonal Operator Basis

Here we describe the change from the operator basis, where the current-current operators are defined as in Reference [4, 12], to the diagonal basis, as defined in [13] (and in this work). The transformation matrices R , M , U , and V in the notation of (A.17) are now given by [4, 13]⁹

$$R = \begin{pmatrix} 1 & \frac{2}{3} & 0 & 0 & 0 & 0 \\ -1 & \frac{1}{3} & 0 & 0 & 0 & 0 \\ 0 & 0 & 1 & 0 & 0 & 0 \\ 0 & 0 & 0 & 1 & 0 & 0 \\ 0 & 0 & 0 & 0 & 1 & 0 \\ 0 & 0 & 0 & 0 & 0 & 1 \end{pmatrix}, \quad M_{ij} = \begin{cases} 1, & i = j, \\ 20, & (i, j) \in \{(9, 1), (10, 2)\}, \\ 0, & \text{otherwise;} \end{cases} \quad (\text{A.35})$$

$$U_{ij} = \begin{cases} 4, & (i, j) \in \{(1, 1), (2, 2)\}, \\ 144, & (i, j) \in \{(5, 1), (6, 2)\}, \\ 0, & \text{otherwise;} \end{cases} \quad V_{ij} = \begin{cases} 4, & (i, j) \in \{(1, 1), (2, 2)\}, \\ \frac{3712}{25}, & (i, j) = (5, 1), \\ \frac{8032}{25}, & (i, j) = (6, 2), \\ 0, & \text{otherwise;} \end{cases}$$

and the matrix W vanishes. These matrices correspond to the following bases of operators (the roles of the primed and unprimed set of operators is reversed with respect to Reference [13]):

$$Q' = (Q_+, Q_-), \quad E' = (E_1^{qq'}, E_2^{qq'}, E_3^{qq'}, E_4^{qq'}), \quad (\text{A.36})$$

and

$$Q = (Q_1, Q_2), \quad E = (E_1^{(1)}, E_2^{(1)}, E_1^{(2)}, E_2^{(2)}). \quad (\text{A.37})$$

All necessary renormalisation constants can be found in Reference [4]. The finite renormalisation is then given by

$$Z'_{QQ}{}^{(1,0)} = \begin{pmatrix} -\frac{5}{3} & -\frac{8}{9} & 0 & 0 & 0 & 0 \\ -4 & 0 & 0 & 0 & 0 & 0 \\ 0 & 0 & 0 & 0 & 0 & 0 \\ 0 & 0 & 0 & 0 & 0 & 0 \\ 0 & 0 & 0 & 0 & 0 & 0 \\ 0 & 0 & 0 & 0 & 0 & 0 \end{pmatrix}, \quad Z'_{QQ}{}^{(2,0)} = \begin{pmatrix} -\frac{29123}{900} - \frac{25}{54}f & \frac{17}{135} - \frac{20}{81}f & 0 & \frac{11}{27} & 0 & 0 \\ -\frac{343}{30} - \frac{10}{9}f & -\frac{498}{25} & 0 & -\frac{4}{9} & 0 & 0 \\ 0 & 0 & 0 & 0 & 0 & 0 \\ 0 & 0 & 0 & 0 & 0 & 0 \\ 0 & 0 & 0 & 0 & 0 & 0 \\ 0 & 0 & 0 & 0 & 0 & 0 \end{pmatrix}. \quad (\text{A.38})$$

⁹Here we have implicitly corrected some typos in Ref. [13].

References

- [1] J. H. Christenson, J. W. Cronin, V. L. Fitch and R. Turlay, “Evidence For The 2 Pi Decay Of The $K(2)0$ Meson,” *Phys. Rev. Lett.* **13** (1964) 138.
- [2] C. Amsler *et al.* [Particle Data Group], “Review of particle physics,” *Phys. Lett. B* **667** 1 (2008) and 2009 partial update for the 2010 edition .
- [3] A. J. Buras, D. Guadagnoli and G. Isidori, “On ϵ_K beyond lowest order in the Operator Product Expansion,” arXiv:1002.3612 [hep-ph].
- [4] M. Gorbahn and U. Haisch, “Effective Hamiltonian for non-leptonic $|\Delta F| = 1$ decays at NNLO in QCD,” *Nucl. Phys. B* **713** (2005) 291 [arXiv:hep-ph/0411071].
- [5] A. I. Vainshtein, V. I. Zakharov, V. A. Novikov and M. A. Shifman, “Processes Of The Second Order In The Weak Interaction In Asymptotically Free Strong Interaction Theories,” *Sov. J. Nucl. Phys.* **23** (1977) 540 [*Yad. Fiz.* **23** (1976) 1024]. F. J. Gilman and M. B. Wise, “ $K_0 - \bar{K}_0$ Mixing In The Six Quark Model,” *Phys. Rev. D* **27** (1983) 1128. J. M. Flynn, “QCD Correction Factors for $K_0 - \bar{K}_0$ Mixing for Large top Quark Mass,” *Mod. Phys. Lett. A* **5** (1990) 877. A. Datta, J. Frohlich and E. A. Paschos, “Quantum Chromodynamic Corrections for $\Delta F = 2$ Processes in the Presence of a heavy top Quark,” *Z. Phys. C* **46** (1990) 63.
- [6] S. Herrlich and U. Nierste, “Enhancement of the $K_L - K_S$ mass difference by short distance QCD corrections beyond leading logarithms,” *Nucl. Phys. B* **419** (1994) 292 [arXiv:hep-ph/9310311].
- [7] S. Herrlich and U. Nierste, “The Complete $|\Delta S| = 2$ Hamiltonian in the Next-To-Leading Order,” *Nucl. Phys. B* **476** (1996) 27 [arXiv:hep-ph/9604330].
- [8] A. J. Buras, M. Jamin and P. H. Weisz, “Leading and Next-to-leading QCD Corrections to the ϵ Parameter and $B_0 - \bar{B}_0$ Mixing in the Presence of a Heavy top Quark,” *Nucl. Phys. B* **347** (1990) 491.
- [9] J. Laiho, E. Lunghi and R. S. Van de Water, “Lattice QCD inputs to the CKM unitarity triangle analysis,” *Phys. Rev. D* **81** (2010) 034503 [arXiv:0910.2928 [hep-ph]].
- [10] O. Cata and S. Peris, “Kaon mixing and the charm mass,” *JHEP* **0407** (2004) 079 [arXiv:hep-ph/0406094].
- [11] J. Brod and M. Gorbahn, in preparation
- [12] K. G. Chetyrkin, M. Misiak and M. Munz, “ $|\Delta F| = 1$ nonleptonic effective Hamiltonian in a simpler scheme,” *Nucl. Phys. B* **520** (1998) 279 [arXiv:hep-ph/9711280].

- [13] A. J. Buras, M. Gorbahn, U. Haisch and U. Nierste, “Charm quark contribution to $K^+ \rightarrow \pi^+ \nu \bar{\nu}$ at next-to-next-to-leading order,” JHEP **0611** (2006) 002 [arXiv:hep-ph/0603079].
- [14] C. Bobeth, M. Misiak and J. Urban, “Photonic penguins at two loops and m_t -dependence of $\text{BR}(B \rightarrow X_s l^+ l^-)$,” Nucl. Phys. B **574** (2000) 291 [arXiv:hep-ph/9910220].
- [15] S. Herrlich and U. Nierste, “Evanescent operators, scheme dependences and double insertions,” Nucl. Phys. B **455** (1995) 39 [arXiv:hep-ph/9412375].
- [16] K. G. Chetyrkin, M. Misiak and M. Munz, “Beta functions and anomalous dimensions up to three loops,” Nucl. Phys. B **518** (1998) 473 [arXiv:hep-ph/9711266].
- [17] H. Simma, “Equations of motion for effective Lagrangians and penguins in rare B decays,” Z. Phys. C **61** (1994) 67 [arXiv:hep-ph/9307274].
- [18] S. A. Larin, “The Renormalization Of The Axial Anomaly In Dimensional Regularization,” Phys. Lett. B **303** (1993) 113 [arXiv:hep-ph/9302240].
- [19] O. V. Tarasov, “Anomalous Dimensions Of Quark Masses In Three Loop Approximation,”
- [20] O. V. Tarasov, A. A. Vladimirov and A. Y. Zharkov, “The Gell-Mann-Low Function Of QCD In The Three Loop Approximation,” Phys. Lett. B **93** (1980) 429.
- [21] S. A. Larin and J. A. M. Vermaseren, “The Three Loop QCD Beta Function And Anomalous Dimensions,” Phys. Lett. B **303** (1993) 334 [arXiv:hep-ph/9302208].
- [22] W. Wetzel, “Minimal Subtraction And The Decoupling Of Heavy Quarks For Arbitrary Values Of The Gauge Parameter,” Nucl. Phys. B **196** (1982) 259.
- [23] W. Bernreuther and W. Wetzel, “Decoupling of heavy quarks in the minimal subtraction scheme,” Nucl. Phys. B **197** (1982) 228 [Erratum-ibid. B **513** (1998) 758].
- [24] W. Bernreuther, “Decoupling Of Heavy Quarks In Quantum Chromodynamics,” Annals Phys. **151** (1983) 127.
- [25] K. G. Chetyrkin, B. A. Kniehl and M. Steinhauser, “Decoupling relations to $\mathcal{O}(\alpha_s^3)$ and their connection to low-energy theorems,” Nucl. Phys. B **510** (1998) 61 [arXiv:hep-ph/9708255].
- [26] P. Nogueira, “Automatic Feynman graph generation,” J. Comput. Phys. **105**, 279 (1993).
- [27] R. Harlander, T. Seidensticker and M. Steinhauser, “Complete corrections of $\mathcal{O}(\alpha\alpha_s)$ to the decay of the Z boson into bottom quarks,” Phys. Lett. B **426** (1998) 125 [arXiv:hep-ph/9712228]; T. Seidensticker, “Automatic application of successive asymptotic expansions of Feynman diagrams,” arXiv:hep-ph/9905298.

- [28] M. Steinhauser, “MATAD: A program package for the computation of massive tadpoles,” *Comput. Phys. Commun.* **134**, 335 (2001) [arXiv:hep-ph/0009029].
- [29] J. A. M. Vermaseren, “New features of FORM,” arXiv:math-ph/0010025.
- [30] F. V. Tkachov, “A Theorem On Analytical Calculability Of Four Loop Renormalization Group Functions,” *Phys. Lett. B* **100**, 65 (1981).
- [31] K. G. Chetyrkin and F. V. Tkachov, “Integration By Parts: The Algorithm To Calculate Beta Functions In 4 Loops,” *Nucl. Phys. B* **192**, 159 (1981).
- [32] A. I. Davydychev and J. B. Tausk, “Two loop selfenergy diagrams with different masses and the momentum expansion,” *Nucl. Phys. B* **397**, 123 (1993).
- [33] T. Hahn, “Generating Feynman diagrams and amplitudes with FeynArts 3,” *Comput. Phys. Commun.* **140** (2001) 418 [arXiv:hep-ph/0012260].
- [34] [Tevatron Electroweak Working Group and CDF Collaboration and D0 Collab], “Combination of CDF and D0 Results on the Mass of the Top Quark,” arXiv:0903.2503 [hep-ex].
- [35] M. Antonelli *et al.* [FlaviaNet Working Group on Kaon Decays], “Precision tests of the Standard Model with leptonic and semileptonic kaon decays,” arXiv:0801.1817 [hep-ph].
- [36] K. G. Chetyrkin, J. H. Kuhn, A. Maier, P. Maierhofer, P. Marquard, M. Steinhauser and C. Sturm, “Charm and Bottom Quark Masses: an Update,” *Phys. Rev. D* **80** (2009) 074010 [arXiv:0907.2110 [hep-ph]].
- [37] K. G. Chetyrkin, J. H. Kühn and M. Steinhauser, “RunDec: A Mathematica package for running and decoupling of the strong coupling and quark masses,” *Comput. Phys. Commun.* **133** (2000) 43 [arXiv:hep-ph/0004189].
- [38] G. Buchalla, A. J. Buras and M. E. Lautenbacher, “Weak decays beyond leading logarithms,” *Rev. Mod. Phys.* **68** (1996) 1125 [arXiv:hep-ph/9512380].
- [39] A. J. Buras and D. Guadagnoli, “Correlations among new CP violating effects in $\Delta F = 2$ observables,” *Phys. Rev. D* **78** (2008) 033005 [arXiv:0805.3887 [hep-ph]].
- [40] A. J. Buras, M. Jamin, M. E. Lautenbacher and P. H. Weisz, “Effective Hamiltonians for $\Delta S = 1$ and $\Delta B = 1$ nonleptonic decays beyond the leading logarithmic approximation,” *Nucl. Phys. B* **370** (1992) 69 [Addendum-ibid. B **375** (1992) 501].
- [41] M. Ciuchini, E. Franco, G. Martinelli and L. Reina, “The $\Delta S = 1$ effective Hamiltonian including next-to-leading order QCD and QED corrections,” *Nucl. Phys. B* **415** (1994) 403 [arXiv:hep-ph/9304257].